Electro-active polymer hydrogels exhibit emergent memory when embodied in a simulated game environment

Article

Published Version

Creative Commons: Attribution-Noncommercial-No Derivative Works 4.0

Open Access

It is advisable to refer to the publisher's version if you intend to cite from the work. See Guidance on citing.

To link to this article DOI: http://dx.doi.org/10.1016/j.xcrp.2024.102151

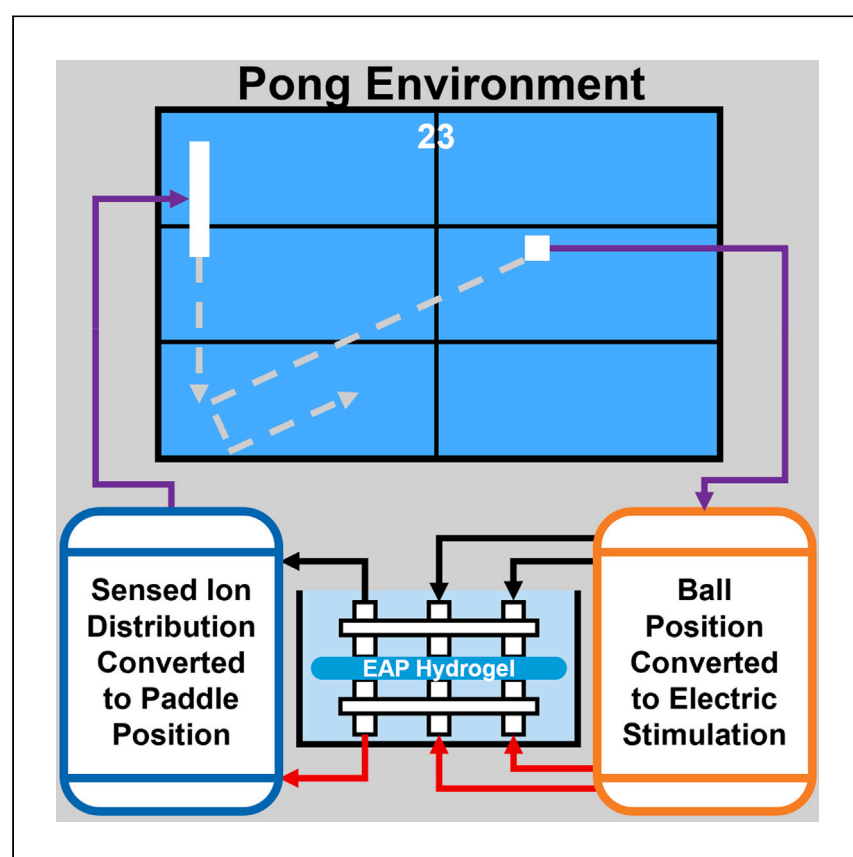Publisher: Elsevier

www.reading.ac.uk/centaur

CentAUR

Central Archive at the University of Reading

Reading's research outputs online

Article

Electro-active polymer hydrogels exhibit emergent memory when embodied in a simulated game environment

Strong et al. demonstrate the application of ionic electro-active polymer hydrogels to computational tasks through use of a multi-electrode array integrated with a simulated Pong environment, taking advantage of the unique memory mechanics present in many active mediums. Improved performance is shown within the task as environmental memory is acquired.

Vincent Strong, William Holderbaum, Yoshikatsu Hayashi

y.hayashi@reading.ac.uk

Highlights

EAP gel memory mechanics are demonstrated via ion concentration measurements

A hybrid EAP gel control system is integrated into a simulated Pong environment

The system shows improved performance over time, supported by control experiments

This demonstrates the application of alternate active medium to computational tasks

Cell Reports
Physical Science

Article

Electro-active polymer hydrogels exhibit emergent memory when embodied in a simulated game environment

Vincent Strong,[1] William Holderbaum,[1] and Yoshikatsu Hayashi[1,2,*]

SUMMARY

The goal of artificial neural networks is to utilize the functions of biological brains to develop computational algorithms. However, these purely artificial implementations cannot achieve the adaptive behavior found in biological neural networks (BNNs) via their inherent memory. Alternative computing mediums that integrate biological neurons with computer hardware have shown similar emergent behavior via memory, as found in BNNs. By applying current theories in BNNs, can emergent memory functions be achieved with alternative mediums? Electro-active polymer (EAP) hydrogels were embedded in the simulated game-world of Pong via custom multi-electrode arrays and feedback between motor commands and stimulation. Through performance analysis within the game environment, emergent memory acquisition was demonstrated, driven by ion migration through the hydrogels.

INTRODUCTION

Emergent computing is a field inspired by the computation that takes place throughout nature and is described as highly complex processes arising from the cooperation of many simple processes[1] or when the behavior of a system does not depend on its individual parts but on their relationships to one another.[2] Artificial neural networks were developed based on the emergent computing behavior of biological brains. Both are large complex systems composed of simple machines whose combined interactions lead to complex computation or thought. The expansion of these theories led to reservoir computing and the application of physical non-linear systems, called reservoirs, as part of the computation process. By using reservoirs found in nature, reservoir computing techniques allowed the emergent computation of nature to be utilized in practical applications; for example, with water ripples for image analysis,[3,4] mycelium mold as maze solvers,[5] and chemical reactors as logic gates.[6,7] These systems solve calculation tasks and often provide unexpected solutions. However, they do not exhibit emergent memory and, by association learning, behavior observed within biological neural networks (BNNs). With limited memory, a reservoir system's capability to improve is limited. This would mean that continuous tasks, requiring behavior based on task history, are too complex for a reservoir to yield any useful result. However, not all possible reservoir mediums behave in this way. With the correct combination of task and computational medium, can emergent memory functions, similar to those observed in BNNs, be achieved? Furthermore, would this allow more complex and nuanced tasks to be pursued through reservoir computing techniques?

To harness the computational power of BNNs, for calculation problems, the field of artificial neural networks (ANNs) was developed. ANNs were created through the

[1]Department of Biomedical Sciences and Biomedical Engineering, School of Biological Sciences, University of Reading, Reading, Berkshire RG6 7BE, UK

[2]Lead contact

*Correspondence: y.hayashi@reading.ac.uk

https://doi.org/10.1016/j.xcrp.2024.102151

application of structural elements from biological brains, with the goal of achieving similar learning capabilities. ANNs have made great strides in solving problems via machine learning that were previously thought to be impossible via computers. However, these solutions are limited by hardware implementation;[8,9] as approximations of BNNs, ANNs are not capable of the learning found in their biological inspiration. Learning behavior, in biological systems, is dependent on the ability of a system to remember the outcomes and consequences of previous iterations within a task.

To better understand how the interactions of biological neurons allow for such complex and useful behavior, theories of morphological and embodied cognition were employed,[10,11] both exploring the integration of computing behavior with the physical "hardware."[12] Embodied cognition theorizes that a body's environmental interactions constitute or contribute to cognition, meaning that memory and learning behavior results from the method of information acquisition, thus resulting from its physical structure.[13] Both theories contribute to the idea that, to achieve the behavior of BNNs in ANNs, hardware capable of the complex interactions present in BNNs is needed. The concept of ANN implementation outside of digital hardware led to the development of reservoir computing.

Reservoir computing derives from recurrent neural network frameworks. The dynamics of a fixed non-linear system, called a reservoir, are used as part of a neural network, mapping input and output signals to higher dimensional space.[14] Reservoirs are typically physical systems exhibiting complex behavior used to encode data, embodying computation not possible within a typical ANN structure. Reservoir computer structures consist of three main layers: an excitation layer, reservoir, and readout layer. The excitation layer encodes network input into reservoir stimulation. The readout layer interprets reservoir responses into usable data, using weights to allow performance tuning and optimization. The reservoir can be any kind of medium that encodes temporal problems into higher dimensions, creating recurrent connections in data.[15]

A promising application of reservoir computing to achieve biological computational capabilities is through biological neurons themselves.[16] Integration of neuron cultures and electronic interfaces produces computational devices[17] referred to as organic or "wetware" computers. By stimulating BNNs with encoded task information, neurons will form pathways in response. This leads to a complex integration of memory in computation via neural plasticity.[18] Wetware computers are usually implemented through control of network plasticity, achieved via application of patterned or random stimulation.[19] By controlling plasticity, the rate of network reorganization is controlled. A feedback loop is implemented where the network is "punished" by increasing plasticity or "rewarded" by reducing plasticity,[19,20] directly influencing what stimulus is incorporated into memory. Implementations of this technology include simulated flight control[21] and the arcade game Pong.[22]

In a previous study,[22] a hybrid BNN-computer system was developed. Using this hybrid system, a grown culture of neurons is trained to play the game Pong in a virtual environment. The game environment is encoded into BNN stimulation with regions designated for ball position sensing and paddle motor commands. Using rally lengths, maximum score before a miss, as the performance metric with a closed loop that manages neural plasticity, the BNN (referred to as DishBrain) improved in ability while playing the game.

Cell Reports
Physical Science
Article

In the hybrid BNN-computer system,[22] supervised learning techniques were used to train the BNN memory for a given purpose. Using random or patterned neural stimulation as punishment or reward, respectively, controls neural plasticity. This method of controlled plasticity is derived from theories of emergent intelligent behavior in biological brains via the free energy principle (FEP).[23–25]

Theories of FEP generally present in BNNs through self-organization of synaptic pathways via active inference,[23,26] although there are many complex layered systems within the brain that can be influenced by theories of FEP. Active inference as a theory holds that the internal structure of the medium represents information about the environment, acting as a form of "memory."[23,27,28] Due to the variable nature of such media, the information is not stored as a one-to-one comparison but as an encoded and pseudo-representative structure. The "memory" continually updates its structure as information is received. As sensed inputs, different from those represented via the structure, are received, free energy increases. The system seeks to reduce free energy by the most direct means. This presents as self-organization and restructuring of the medium.[29,30]

Since the initial theories presented through the DishBrain studies,[22] other concepts have come to expand on the role of free energy and self-organization within systems of memory, both in and outside of biology. The most impactful so far is that of criticality.[31]

Dynamic criticality consists of many ideas applied on the basis that the medium, such as a BNN, is a type of excitable, or active, medium and, in a broader sense, a dissipative dynamical system. To briefly summarize, theories of criticality posit that these systems, when provided with energy, evolve into a "critical state" in which interactions are no longer subject to characteristic time or length scales,[32,33] effectively bridging the gap between local and global scales of interaction. This loss of scale presents spatially as self-reorganization, resulting in the emergence of scale-invariant, or fractal, structures[33–35] representative of the method in which the energy was provided. The co-dependency of FEP and criticality[36] was further expanded on in work by Isomura et al.[36] In this study, BNN cultures were trained on mixed sensory input from two sources. Through reverse engineering techniques, they were able to predict the reorganization of the BNN through the minimization of variational free energy, as the sensory input was encoded into the structure or "memory."

However, BNNs are not the only medium that presents restructuring behavior that could be conceptualized via theories of free energy for the purpose of computation. Many active-matter materials also display these mechanics.[37] Ionic electro-active polymer (EAP) hydrogels are active materials also governed by these principles, with ions migrating under the influence of electric fields to reduce system free energy,[38] reorganizing the ion distribution to adapt to the temporal and spatial pattern of electric stimulation.

Ionic EAP hydrogels are active-matter materials[39] showing promise in soft robotics as actuators.[40] Recent studies have shown the potential for these materials to be used in computation,[41] given an appropriate application and framework. This material changes shape in response to electric stimulation, with ions acting as active agents. The dynamics of these active particles have shown memory-like behavior.[42] Electric stimulation increases free energy, which, via ion migration, the EAP seeks to minimize.[38] This migration causes a restructuring of the EAP's distribution of ions and charged polymer chains. The method of information encoding via ion migration

is comparable to the role of ions within the neurons of the BNN, where the inhomogeneous distribution of ions appears as a common driving mechanic.

Therefore, if the EAP's electric stimulation was representative of an environment, then would the reorganization of ions be representative of that environment, similar to the structure of BNNs within the brain? Furthermore, if both ionic EAPs and BNNs exhibit memory behavior, then is it possible that EAPs, like BNNS, can exhibit improved motor performance via memory if applied to an established BNN task such as Pong?

In summary, there are many computation techniques that are being developed rapidly to achieve the kind of emergent memory behavior found in BNNs. Theories in embodied computation have led to developments in ANNs, allowing physical media with complex behaviors to be used as computational resources.[14] Through reservoir computing, BNNs were integrated into computational tasks using fundamental theories of free energy[14,22] that were then expanded on through theories of criticality.[31,36]

This study aims to show how EAP hydrogels can exhibit emergent memory functions when embodied in a simulated game environment. First, by measuring ion concentrations through conductivity of the EAP hydrogel after periods of electric stimulation, the memory mechanics of the ionic EAP hydrogel were studied. Second, the EAP hydrogel was embodied in the simulated game environment of Pong through a custom multi-electrode array (MEA). The game Pong was used as an established task for this study via current work in wetware computers.[22] The game environment was encoded into stimulations provided to the hydrogel, and recorded ion concentrations were used as motor commands. Multiple game "runs" were conducted with this setup, with game performance over time recorded and analyzed in order to determine the effectiveness of the system's "memory" within the task.

RESULTS AND DISCUSSION

Memory mechanics through ion migration and conductivity measurement

For a medium to be used in computation, it must exhibit behaviors representative of properties key to the computational system; the most fundamental of this is memory. Polyacrylamide hydrogel is an ionic EAP that displays mechanics that can be interpreted as a form of computational memory.

Polyacrylamide hydrogel is an active-matter EAP;[38] hydrogen ions act as active agents within the hydrogel, influenced by the polymer network and each other. Stimulation by an electric field causes an increase in free energy within the hydrogel, and the ions migrate[43] to minimize the free energy of the system.[38] As the ions move, they drag water molecules, causing changes in water distribution and localized deformation of the gel, driven by an equilibrium between osmotic pressure[44] and rubber elasticity[45] in the polymer network. Given a constant migration of ions into a location, the localized rate of swelling gradually decreases, further decreasing free energy. This creates a hysteresis effect[46] that leads to complex dynamics in the gel's reactions to stimulation.

The hydrogen ions take relatively little time to migrate under stimulation by an electric field but take considerably longer to diffuse to a homogeneous distribution under no stimulation. The difference in timescale allows previous stimulations to affect future stimulations, as the ion distributions persist between stimulations, leading to a form of memory.[42,47]
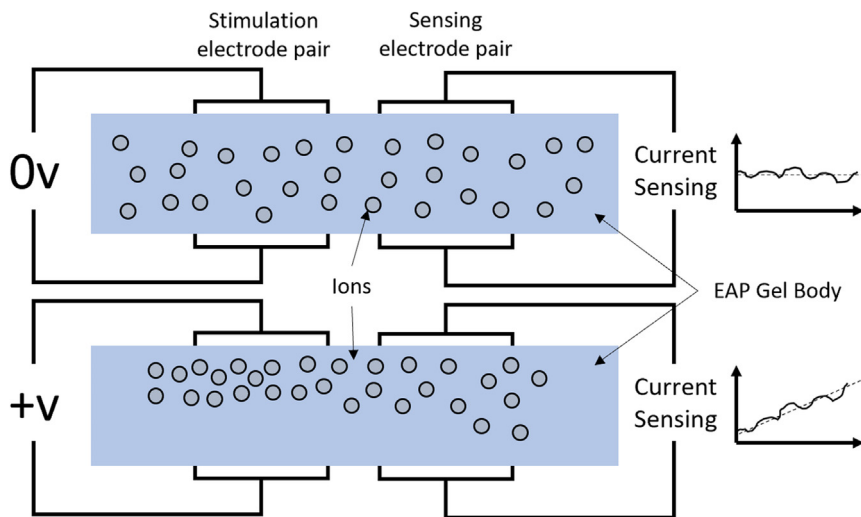
Figure 1. Ion motion under electric stimulation

Diagrams show how ion motion is influenced by external stimulation via an electric field and recorded via electric current draw. Under stimulation, ions will gather between the electrode pair from elsewhere in the EAP gel. As the concentration of ions in this location increases, the conductivity also increases; the increase in conductivity can be measured as an increase in electric current draw when a small voltage is applied in parallel close to this location via a secondary electrode pair.

This experiment is designed to demonstrate this initial memory mechanic and detail the underlining methodology that is used in the subsequent experiment presented in this study regarding the impact of said memory. By recording the ion concentrations before and after consecutive stimulations, the "remembered" state caused by the stimulation can be observed. Ion concentration can be measured through the conductivity of the gel. As ions collect in a location and ionic concentration increases, the local conductivity also increases.[48] By applying a small voltage to said location, the electric current draw on the power supply is directly proportional to the conductivity and, thus, directly proportional to the ion concentration. By utilizing two adjacent pairs of electrodes, stimulation can be applied while conductivity is measured simultaneously. This setup is illustrated in Figure 1.

To better understand hydrogel EAP system behavior, as shown in Figure 1, the basic mechanisms can be described through Frick's first law of particle diffusion,[49] characterizing diffusive flux J over a free energy gradient δu, shown in Equation 1. There are three main components to the free energy u of ions within the hydrogel system, shown in Equation 2:

(1) energy due to the electric field imposed by the electrode pair u_e,
(2) energy imposed by the changing chemical concentration gradient within the hydrogel as ions migrate u_c, and
(3) energy due to the electrical potential gradient of ions within the hydrogel as ions migrate u_p.

u_e and $u_c + u_p$ (electrochemical gradient) oppose each other. As the electric field attracts ions to a location, the local concentration and potential increase, causing an increase in free energy opposing that of the electric field:

$$J = \frac{D}{RT}\frac{\delta u}{\delta x}$$ (Equation 1)

where

$$\delta u \ = \ u_e + u_c + u_p \qquad \text{(Equation 2)}$$

$$u_e \ = \ k_e \frac{v\epsilon Ae}{dr} \qquad \text{(Equation 3)}$$

$$u_c \ = \ RT \ln\left(\frac{m_2}{m_1}\right) \qquad \text{(Equation 4)}$$

$$u_p \ = \ ZF(v_1 - v_2) \qquad \text{(Equation 5)}$$

u_e can be represented via Coulomb's law and electric potential energy, shown in Equation 3. Ion charge is equal to electron charge; the charge imposed by the electrode pair is derived from the capacitance of the electrodes surrounding the hydrogel. u_c can be derived from the Gibbs free energy representation of thermodynamic entropy as the ratio between concentration increases,[50] shown in Equation 4. u_p is represented via the Gibbs free energy derivation of cell potential as the combined charge of ions becomes inhomogeneous,[50] shown in Equation 5.

Due to Coulomb's law, as the ions approach the charged electrode pair, u increases, resulting in a larger flux J. However, $u_c + u_p$ also increases opposing the electric field. These two opposing forces change at very different rates, with the difference in magnitude being a key factor of the hysteresis component. As the ions migrate under the influence of the electric field, eventually the u is minimized as the opposing factors balance. This interpretation is, however, a simplification. In actuality, there are many additional free energy components that contribute to the complexity of the hydrogel's EAP behavior, such as terms associated with the deformation of the gel's polymer structure as it swells due to local ion and water concentrations. These additional terms also influence factors of other terms, such as diffusion coefficients and permittivity of the hydrogel material, resulting in extremely complex behavior as the free energy is minimized.

Experimental approach
Using these concepts, a series of stimulations were applied to a polyacrylamide hydrogel sample to demonstrate the memory mechanism. Polyacrylamide is a relatively simple EAP hydrogel to synthesize,[51] allowing for it to be produced in large batches and molded in many different ways for the required experiments. The gels were synthesized using the methodology described in the supplemental experimental procedures under "Gel synthesis procedure." The gel was left in a sodium chloride solution (0.08%) to allow the ion concentrations to stabilize and provide a consistent starting water concentration within the hydrogel. The gel was then placed between two electrode pairs spaced with a 7 mm gap between them. A constant sensing voltage of 2 V was applied to one electrode pair, using an electric current sensor to record the response, while a series of 20 V stimulations, across the thickness of the hydrogel (8.5 mm), was applied to the second electrode pair. Both voltages were applied with the same polarity.

Temperature and water content within the hydrogel can affect free energy equilibrium.[38] Temperature alters the elastic properties and rate of ionic motion.[51] As the osmotic pressure difference between the polymer networks and ionic solution drives the swelling, changes in the hydrogel's water content change the degree to which it can swell, as well as altering the mechanical properties of the material.[52] Because of this, temperature and water content must be controlled. To mitigate
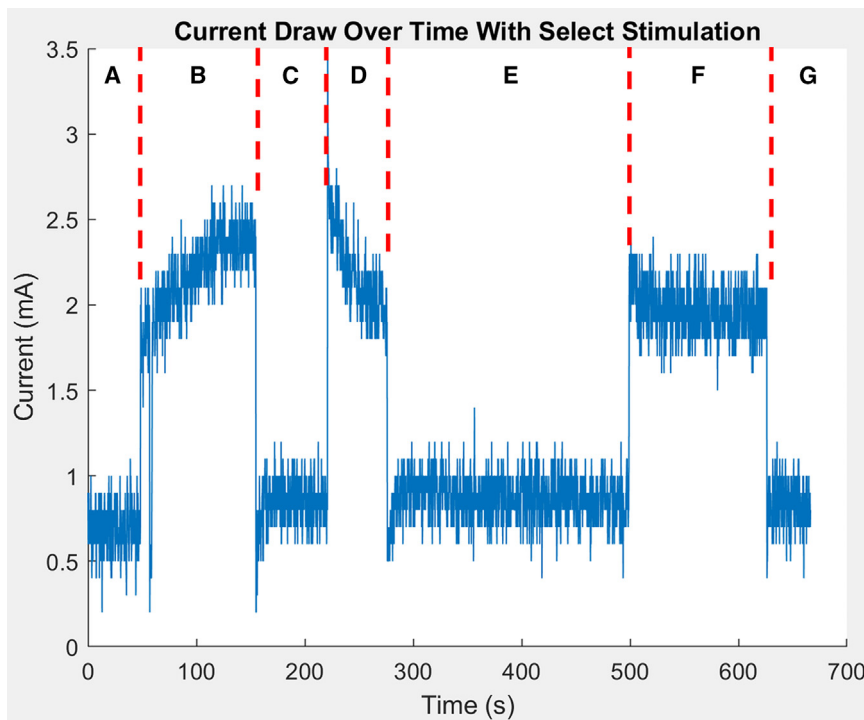
Figure 2. Electric current draw over time with select stimulation

Shown is a sample of a recorded electric current draw from 2 adjacent parallel electrodes as described in Figure 1. The data are segmented and labeled A–G for reference. The sensing voltage (2 V) was applied continually through the entire demonstration, and stimulation (20 V across the 8.5-mm-thick hydrogel) was applied in sections B, D, and F. The recorded electric current has a default value of approximately 0.8 mA, as the EAP gel is inherently conductive, as shown in segment A. With application of an electric field, there is an immediate rise to 2 mA as the field is picked up by the sensing electrode pair shown at the beginning of segment B.

this as much as possible, the water was taken from a temperature-controlled source (approximately 22°C) to ensure that the solution was at a consistent temperature and provide the same starting temperature conditions. Furthermore, the gels were stored in watertight containers and left in the ionic solution for the same period of time to ensure the water content of the hydrogel was consistent.

Findings

The results of this demonstration can be seen in Figure 2. The recorded electric current had a default value of approximately 0.8 mA as the EAP hydrogel was inherently conductive, as shown in segment A. With application of an electric field, there is an immediate rise to 2 mA as the field is picked up by the sensing electrode pair shown at the beginning of segment B. The stimulation also caused an increase in free energy. As a result, the ions moved toward the electrode pair to minimize free energy. The electric current draw rose, as ions collect and conductivity rose, to 2.4 mA, as shown in segment B. Once the stimulation was removed, the electric current dropped back to default values, as shown in segment C. Once the stimulation was reapplied, the electric current draw immediately rose back to the point where segment B ended, as the ions still maintained their positions, as shown at the start of segment D. This observed behavior exhibits a memory-like mechanism where a value is "saved" to the EAP hydrogel by the redistribution of ions within the gel. This behavior can then be seen again at the beginning of segment F, where it continues from where segment D finished.

Interpretation

From this demonstration of memory mechanics, it is evident that changes in the ion distribution and polymer network can be recorded as electric current draw through the application of small voltages. This is evidenced by the change in electric current over time as stimulation is applied, altering the ion distribution and polymer network. The demonstration also highlights how the increase in free energy through stimulation was resolved by the hydrogel through ion migration and the last state of the EAP hydrogel "remembered" after the electric stimulation was removed. With reapplication of the stimulation, the changing electric current continued from the last state recorded during stimulation. From these observations, it can be established that a form of memory is present in the EAP hydrogel, and the response due to the hydrogel's memory can be measured in parallel with the application of stimuli. To fully demonstrate this memory mechanism and its value within computation, a suitable activity was required, along with a closed-loop control structure and hardware to interface with the hydrogel.

EAP hydrogel embodied in a simulated game world

The memory-like behaviors of the EAP hydrogel can be characterized through free energy minimization.[38] There are many systems whose mechanics can be represented through free energy minimization; in computation, one of the most significant is that of BNNs.[23] Furthermore, in the most basic sense, biological brains represent information through the self-organization of neurons as active agents.[53] Similarly, EAP hydrogels can represent information via the distribution and organization of ions as active agents. Information in BNNS is also stored through many other complex means; however, the organization of neurons serves as a leading mechanism within the BNN system. To accurately demonstrate the memory mechanics within a task, the EAP hydrogel must be embodied within a closed control loop, as is present in BNN systems. To induce emergent memory functions, the hydrogel must be able to influence actions within an environment. The change in environment as a result of those actions must feed back to the hydrogel, leading to changes in actions and memory behavior. To construct this closed loop and quantify the effect of memory, a suitable activity is required.

A previous study[22] used a single-player version of the game Pong as the quantifying activity when integrating a BNN with computer architecture. The game provided a virtual environment for the BNN to inhabit and from which to acquire information. The method used to interface the biological neurons with the simulated environment fits neatly with the reservoir computing framework.[14] In the study,[22] the position of the ball was presented to the neurons through localized stimulation, aligning with the function of the excitation layer in a reservoir computer. The neuron responses were converted to motor commands to control the paddle, aligning with the function of the readout layer.

A common driving mechanism between both BNNs and EAP hydrogels is the migration of ions in reaction to stimuli, creating an inhomogeneous distribution of ions throughout the media. Ion migration can encode information provided via stimulation in the sensory-motor loop. As shown in previous work, the resulting inhomogeneous distribution of ions can present as a memory function of previous stimuli.[41] Utilizing a reservoir computing framework, performance of the computational ability within the EAP hydrogel can be assessed using the Pong game-based activity in a simulated game environment.

Experimental approach

An MEA was used to interface the EAP hydrogel with a computer system containing the Pong game environment. The array of electrodes was divided into two regions,
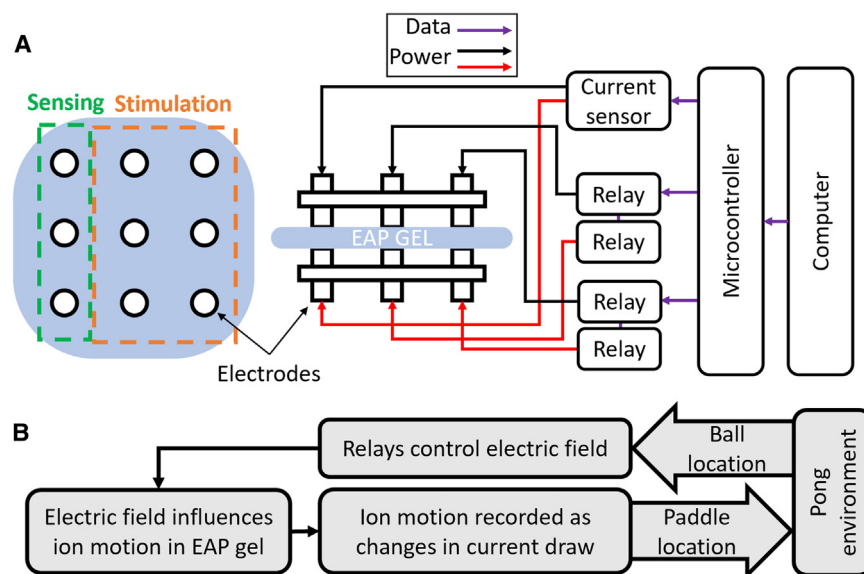
Figure 3. System layout of closed-loop communication between the computer containing the Pong environment and the EAP hydrogel

(A) The layout of communication between components in the system and separation of the electrodes into regions. The electrodes are divided into driving, which provide stimulation, and sensing, which measure electric current draw. The driving electrodes are driven by relays that direct the electric field (20 V across the 10-mm-thick hydrogel disk). The sensing electrodes provide a small voltage (2 V), and the electric current draw is measured by an electric current sensor. Both relays and sensors are coordinated by a microcontroller, which, in turn, is directed by the computer and Pong game environment. A more detailed circuitry schematic can also be found in Figure S1. Additionally, an image of the physical hardware can be seen in Figure S2.

(B) A flowchart of the information path from the Pong environment on the computer to the hydrogel containing the ions.

used to provide a stimulus as input to the gel via the application of electric fields at select locations and record output via the electric current at select locations. This division of regions is similar to how MEAs are currently used in applications.[22,54] By dividing areas into specific tasks, interference from different tasks happening in the same location is minimized. The layout of these regions can be seen in Figure 3A.

The stimulation region of the gel acts as the stimulation layer of the reservoir framework, consisting of a 2 × 3 array. To translate the ball's position into stimulations, the game environment was divided into a 2 × 3 grid, as shown in Figure 4B. The location of the ball in the game environment is sent from the computer to the MEA; as the ball passes through those regions, the corresponding electrode pair is activated to stimulate that area. The regions as they are labeled in black in Figure 4B are how they will be referenced throughout this paper.

The sensing region acts as the readout layer of the reservoir framework. Electric current sensors were used to measure the electric current draw at the sensing electrodes, utilizing the small sensing voltage (2 V) defined in the previous experiment. These electric current values are recorded on screen, shown in Figure 4A, recorded in milliamperes, and interpreted into motor commands for the paddle. Recorded electric current values are normalized using the maximum and minimum electric current values recorded from the hydrogel during the previous experimentation with the apparatus, found to be +3 mA and −0.75 mA, respectively. A trend is then calculated using these normalized values against their locations represented in the Pong
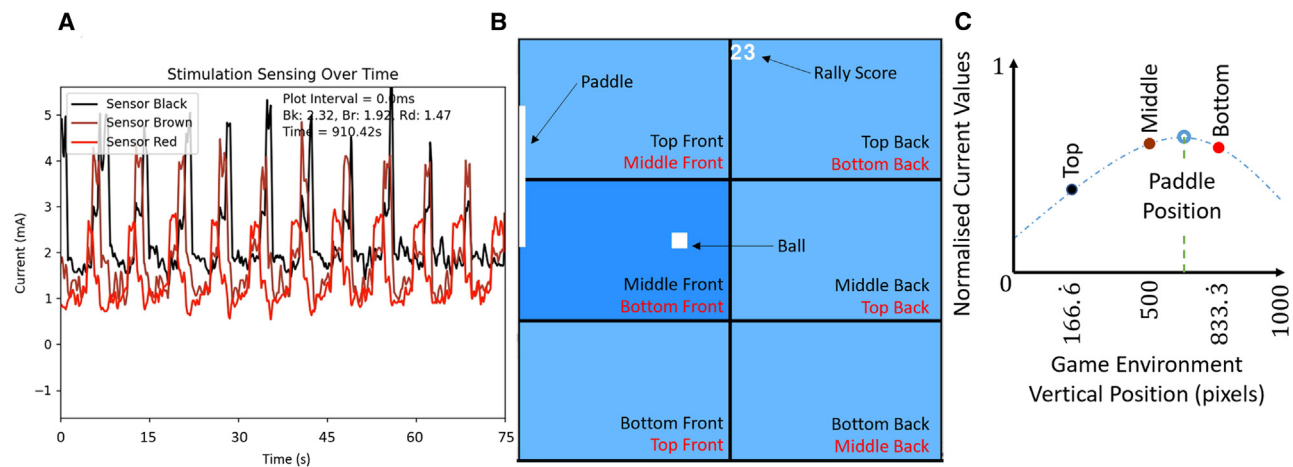
Figure 4. Software representation of the Pong game within the computer

(A) The electric current sensor readings as they are received by the computer. The black, brown, and red lines represent the top, middle, and bottom sensors, respectively. The interval between received data is also measured and averages 0.5 mS, labeled as "Plot Interval." The averaged electric current across the graph for each sensor is measured for the purposes of establishing default values, labeled as "Bk," "Br," and "Rd." The total recording time is also displayed, labeled as "Time." These sensor values move the paddle in the Pong game environment through conversion to a position based on sensor location, as visualized in (C). This can be seen on the computer screen, along with the apparatus shown in Figure S3.

(B) The simulated Pong game environment, 1,000 × 1,000 pixels, which is separated into 6 regions as described in Figure 3B. When the ball is in a region, it will darken, and the corresponding electrode pair will stimulate the EAP hydrogel. The score is displayed at the top and resets when the ball hits the left wall behind the paddle. The regions are also labeled in black here for reference within this paper. The paddle is set to 1/3 the environment height (333 pixels). The rearrangement of regions used for the control dataset, where "vision" is impaired, is indicated by the red labels. This can be seen on the computer screen, along with the apparatus shown in Figure S3.

(C) An example of the method used to place the paddle based on the electric current readings as measured in (A), shown here as the same representative colors and labeled with their region locations. The electric current readings are normalized between 0 and 1 and plotted based on their region's center vertical location. A second-degree polynomial is applied, as indicated by the blue dashed line. The point where the polynomial is at its peak is the maximum predicted electric current, as indicated by the blue circle, and this is where the paddle is placed.

game environment. The trend is generated by fitting a second-degree polynomial to the 3 points. The peak of this trend is the predicted point of highest electric current and highest ion concentration in the gel and is where the paddle is placed. This is illustrated in the example in Figure 4C.

Through this layout of hardware and software, a closed loop was established, where the computer outputs the game's environment, represented as ball location, to the MEA applied to the gel as shaped electric fields. In response, the ion concentrations are measured by the MEA as electric current and provided to the computer and the Pong game to move the paddle. This closed loop is outlined in Figure 3B. A more detailed description of the behavior and implementation of the Pong game, as shown in Figure 4, can be found in Note S1. Similarly, a more detailed description of the hardware implementation, as shown in Figure 3A, can be found in Note S2. A circuitry schematic and image of the physical hardware can be found in Figures S1 and S2. The full setup of the computer game environment and MEA apparatus can be seen in Figure S3. The full experimental procedure for each run of the Pong game with the EAP hydrogel can be found in the supplemental experimental procedures under "Pong Game Experimental Procedure." In total 21, separate EAP hydrogel runs were carried out, collecting 3,500 s of "gameplay" for each run before the hydrogel degraded beyond the point of continuing.

From these games, several metrics were recorded to be used in performance analyses, such as electric current measurements, stimulation positions, and score. The score, shown in Figure 4B, increases whenever the paddle successfully hits the ball
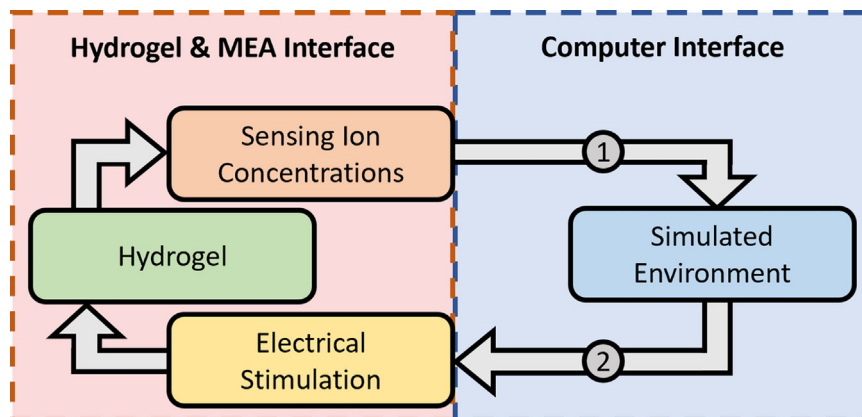
Figure 5. Information flow paths within the experimental setup
Shown is a representation of the flow of information between the MEA and computer systems. The key points of information transduction that can be altered for the purpose of control experiments are labeled as 1 and 2.

and resets to 0 whenever the ball misses the paddle hitting the wall. All data from these separate runs was combined into a single dataset to view the overall averaged behavior of the hydrogel and assess the performance as well as the repeatability.

Control experiments via interference of information translation. A set of control experiments were undertaken to create a baseline against which to compare performance. The primary purpose of the baseline comparison is to further show that the hydrogel's improved performance was a direct result of the closed loop control and based on the accurate information received, such as the position of the ball from the Pong environment. These experiments explore the null hypothesis that the hydrogel's performance increase was not a result of accurate game environment information. The control experiments were designed to accomplish this by interfering with the translation of information between the hydrogel and the simulated game environment. By altering this translation, the hydrogel is presented with information that does not accurately represent the simulated game environment, and, thus, it is expected that the hydrogel would be unable to effectively control a paddle. There are two key positions within the closed feedback loop, between the hydrogel and game environment, that can be altered; these are labeled in Figure 5 and described as follows:

(1) translation from electric current readings in the hydrogels, related to ion concentrations at electrodes, to produce motor commands controlling paddle position within the game environment and
(2) translation from ball position within the game environment to the location of the electric stimulation on the hydrogel via electrodes.

Control experiments can be applied by altering the flow of information within the closed feedback loop at either of these key positions:

(1) altering the flow of information from the hydrogel to the simulated game environment via interfering with the translation of information at point 1 or
(2) altering the flow of information from the simulated game environment to the hydrogel via interfering with the translation of information at point 2.

At these positions in the closed control loop, there are also two main ways in which information translation can be altered: either through the manipulation of mapping

functions, altering the way in which electrode positions in the hydrogel map to positions in the simulated game environment, or by entirely severing the information path. The latter method would, however, only provide useful information in position 2. If position 1 were to be severed, the information used to control the paddle would be the result of noise in the electric current sensors reading unconnected electrodes. This means that the hydrogel itself would have no impact on the actions within the simulated game environment, and therefore, any results would provide no insight into the behavior of the hydrogel within the altered control loop.

In all of these control experiment structures, for the null hypothesis to be rejected, the hydrogel would need to exhibit no adaptation or performance improvement due to memory. For this to be true, the hydrogel performance in the game would need to not increase by any statistically significant amount. This is also true if the hydrogel performs worse than if the paddle was moving randomly. As the paddle is 1/3 the height of the simulated environment, the rejection would require a hit rate below 33% for this condition.

The first control experiment, impairing sensing through remapping (referred to as impaired sensing), was achieved through simulation, utilizing the data collected through running the experiment with hydrogels. Simulation allows for multiple arrangements of sensing inputs to be tested without the need to run experiments with hydrogel samples. The method of simulation is detailed in Note S7. In this control experiment, the electric current sensing regions, as described in Figure 4C, were rearranged from top, middle, bottom to middle, bottom, top. This ensures that all sensing regions are in entirely different areas and ensures that the data collected for each region will not repeat those of the unaltered feedback loop experiment. As the information transfer between the simulated environment and the simulated hydrogel is impaired but not severed, this experiment still represents a closed-loop system. However, as the sensory information is rearranged, the direct effect of the closed loop is impeded.

The second control experiment, impairing stimulation through remapping (referred to as impaired stimulation), however, cannot be accomplished in simulation. Due to the complex interference between stimulated regions within the EAP hydrogel, this experiment must be performed on the hydrogel sample. This was accomplished by rearranging the game environment's regional, or ball's positional, correlation to the MEA's stimulation electrodes. This results in incoherent environmental information to the hydrogel and effectively impairs its "vision" of the ball position. The rearrangement of game environment regions can be seen in Figure 4B, indicated by the red labels. As with the first experiment, the information transfer between the simulated environment and the hydrogel is impaired but not severed; thus, this experiment still represents a closed-loop system. However, as the stimulating information is rearranged the direct effect of the closed loop is impeded.

The third control experiment, severing stimulation (referred to as severed stimulation) was also performed, using the hydrogel samples. This is because, in this experiment, the hydrogel is under no stimulating voltage but is still under sensing voltage, a combination that is not present in any of the other experiments. Because of this, the electric current responses, and by association the paddle positions, cannot be derived, and simulated, from any of the previous experiments. This experiment was accomplished by disconnecting the stimulating electrodes from the MEA, thus preventing the simulated environment from providing any electric stimulation to the hydrogels. The electric currents from the hydrogels were still measured to
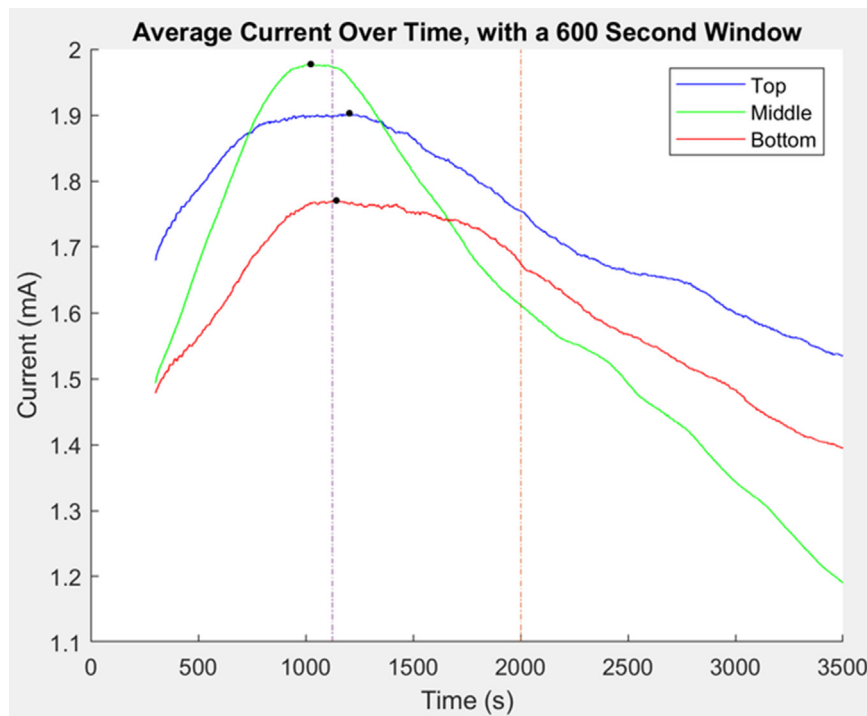
CellPress
OPEN ACCESS

Figure 6. Average electric current over time, with a 600 s window

Shown is the electric current at each sensor over time for the combined unimpaired dataset of runs, smoothed using a moving average window of 600 s. Due to the averaging, data start at 300 s. The point of maximum electric current draw is marked with a black dot; 1,203, 1,023, and 1,142 s for top, middle, and bottom, respectively. The average point of maximum electric current draw is marked by the purple vertical dashed line at 1,122 s. The orange vertical dashed line marks the earliest point the EAP gels broken down. Standard error was calculated for each trend from the windowed samples and found to be at maximum, 0.0169, 0.0053, and 0.0116 for the top, middle, and bottom trends, respectively.

produce motor commands to control the paddle in the Pong game. With the information transfer between the simulated environment and the hydrogel severed, this experiment represents an open-loop variant of the system. The hydrogel's performance within the game is still recorded; however, the change in performance is independent of the information provided by the ball's position within the simulated environment.

Findings
Memory function of the EAP hydrogels via electric current measurement. To show the memory mechanics in the MEA experimental structure, the measured electric current draw was plotted for each sensing electrode pair. Figure 6 represents the combined measured electric current data points of all 21 game runs, with data points sorted against time, averaged using a 600-s moving average window.

The electric current initially rises as ions move toward the electrodes. As the ions accumulate, their rate of migration decreases due to the increasing concentration gradient. Eventually, the ions stop moving, and the electric current reaches its maximum, shown in Figure 6 by the vertical purple dashed line. This gives an initial view of minimized energy in the form of electric current and establishes the time range in which memory acquisition may occur. The electric current then falls as the hydrogel eventually breaks down under the effects of electrolysis,[55] impairing
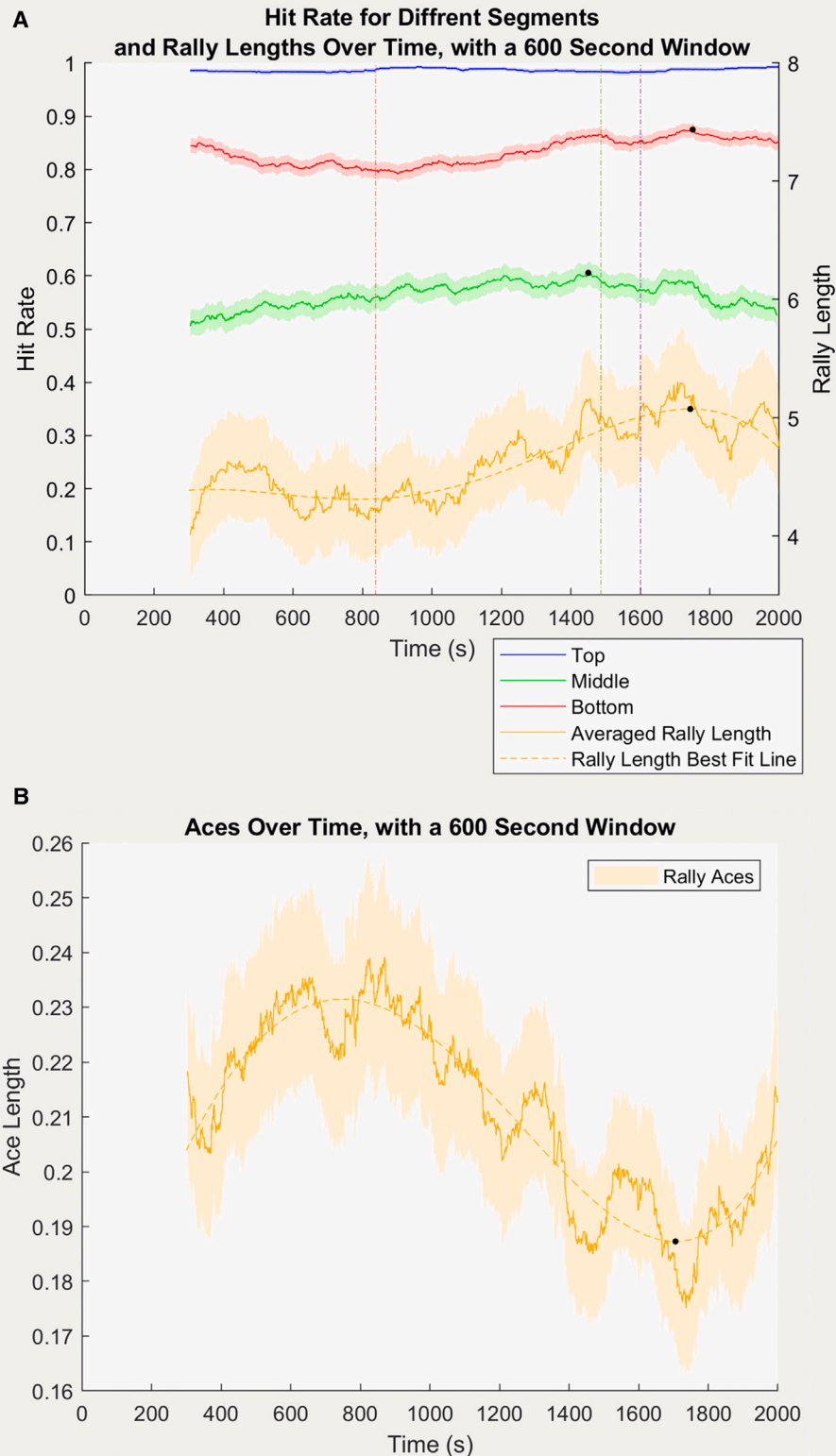
Figure 7. Averaged performance metrics over time

(A) Left axis: the hit rate as a hit-to-miss ratio over time for the combined unimpaired feedback loop dataset, separated based on the region where the hit/miss occurred, as described in Figure 4B. Smoothed using a moving average window of 600 s, this window size provided the clearest view; additional window sizes can be seen in Figure S6. The standard error for each windowed sample is shown by the shaded area. The point of maximum performance is marked on the "Middle" and "Bottom" lines by a black dot; 1,450 and 1,750 s, respectively. The average between these times is marked by the purple vertical dashed line (1,600 s). As seen from the graph, the middle region saw a performance increase of 0.1, from 0.50 to 0.60. The bottom region decreased to 0.79 before increasing to 0.87; from its lowest point, this is a performance increase of 0.08. Right axis: the rally length (maximum score before a miss) against time for the combined unimpaired feedback loop dataset, smoothed using a moving average window of 600 s. The standard error for each windowed sample is shown by the shaded area. A fourth-degree polynomial best fit line was applied via the MATLAB Polyfit function.[56] This was the minimum order polynomial that fit the trend presented by the data. The maximum point of performance is marked by the black dot at 1,744 s. This marks an increase of 0.8, from 4.3 to 5.1. These data, prior to the application of the moving average, was used to perform a one tailed t test. From 0 s to the vertical orange dashed line (838 s) indicates the dataset used to represent before MA. From the vertical green dashed line (1,487 s) to the cutoff of 2,000 s indicates the dataset used to represent after MA. The distributions of these datasets can be seen in Figure S8.

(B) Plot of rally aces, representing the number of times the paddle failed to intercept the ball without a single hit, smoothed using a moving average window of 600 s. The standard error for each windowed sample is shown by the shaded area. A fourth-degree polynomial best fit line was applied via the MATLAB Polyfit function.[56] This was the minimum order polynomial that fit the trend presented by the data. The maximum point of performance is marked by the black dot at 1,706 s. This marks a decrease of 0.04, from 0.23 to 0.19.

connection between electrodes. This breakdown marks a cutoff point that is indicated in Figure 6 by the orange vertical dashed line at 2,000 s. Thus, the graphs used to analyze the hydrogel's performance were limited to between 0 and 2,000 s.

Performance of the EAP hydrogel within the Pong game. To assess the performance of the hydrogel within the Pong game, the hit rate was calculated using the combined data points of the 21 game runs sorted by timestamp, shown in Figure 7A as the left axis. 21 experiments were sufficient for reliable results, shown via standard deviation analysis, described in Note S3. Due to the boundary conditions of the paddle, the top and bottom regions of the wall were hit more often by the ball than the middle (Figure S4). As the hit rate is different between regions, the performance improvement rate may be different between regions. For this reason, the hit/miss data were segmented based on the region in which the hit/miss occurred. Figure 7A shows the segmented paddle performance curve for the top, middle, and bottom game regions.

For the middle region, the paddle had an initial ball hit rate of 50%, but over the course of the game, this rose to maximum of 60%, giving a rise of 10% over 1,450 s. The middle region shows the greatest improvement in performance.

The top and bottom regions are subject to the boundary conditions, leading to a higher initial hit rate, as seen in Figure 7A, as the trend via the measured electric current in those regions is almost linear, as seen in Figure 6. For the bottom region, the paddle initially hit the ball approximately four times more often than it missed, hitting 79% of the time. As the bottom region is also a boundary condition, this is expected. However, over time, this performance did increase up to a maximum of an 87% hit rate, showing an improvement of 8% over 1,750 s.

When compared to the other regions, when the paddle was in the top region, it rarely missed the ball. However, when the successful paddle hits are summed for each region over the 21 game runs, the paddle hit the ball in the top region 49% of the time, while the middle and bottom regions hit the ball 12% and 40% of the time, respectively. This distribution can be found in Figure S5A. This distribution follows the distribution of ball hits as seen in Figure S4, with the top and bottom regions hitting more often, consistent with each other, while the middle region is hitting far less often. This means that the distribution of paddle hits matches the inherent distribution of the game physics and, furthermore, that the increased hit rate is not due

to the ball spending a higher percentage of time in the top region. However, when summing paddle misses, the top region has far fewer occurrences across all experiments. The paddle, when in the top region, only missed the ball 4% of the time, while the middle and bottom regions accounted for 66% and 30% of misses, respectively. This distribution can be found in Figure S5B. This means that the comparatively high hit rate of the top region is, in actuality, caused by a much lower miss rate than the middle or bottom regions.

From the readings shown in Figure 6, the top sensor tended to read higher electric currents than the other regions. These higher electric current readings, and, by connection, the lower miss rate, are likely due to some bias in the MEA rig construction. However, this bias was consistent through all experiments, including the control experiments. It should also be noted that the ball hit locations are distributed randomly across the "goal" of the game environment; this is supported by the measurement of hit distributions shown in Figures S4 and S5. Similarly, the ball's speed and direction are seeded randomly at the start of each game; this is explained in Note S1. Because of this, the bias should pose no long-term implications within the results gathered.

As shown in Figure 7A, when in the bottom region, the paddle initially hit the ball approximately four times more often than it missed, hitting 79% of the time. As the bottom region is also a boundary condition, this is expected. However, over time, this performance did increase up to a maximum of an 87% hit rate, showing an improvement of 8% over 1,750 s.

To better show the overall performance increase through the course of the game, a graph was generated of the rally lengths against time via the right axis. The rally length is a measure of how many times the ball was hit before it was missed, shown as the "rally score" in Figure 4B. The score reached before it resets to zero when missed is called the rally length. Each time the ball was missed, the rally length achieved was recorded against the time and plotted using an averaging window of 600 s as with the previous plots. Figure 7A shows an increase in rally length over the course of the game. The metric appears to fluctuate more than the hit rate; however, this is due to differences in scale and averaging over the combined scores of many samples, leading to higher variation. This does not impact the conclusion gathered from these results, as the standard error follows the same trend. This graph clearly shows the ability of the gel to perform within the Pong game before and after information of the simulated environment has been integrated into memory, referred to in this study as memory acquisition (MA). With this separation of states, before and after MA, the significance of the increase in the hydrogel-controlled paddle's performance, via the rally lengths, can be analyzed.

The significance of the change in performance can be analyzed through a statistical test (using null hypothesis $\alpha = 0.05$) between the rally length before and after the performance increase via MA. The sample representing before MA was subsampled from 0 to 838 s in the rally length dataset, shown via the vertical orange dashed line in Figure 7A. The sample representing after MA was a subsampled from 1487 to 2000 s in the rally length dataset, shown via the vertical green dashed line in Figure 7A. Details on how these ranges were selected can be found in Note S4.

Although the pre and post MA values were recorded from the same gel samples, these values were recorded when the hydrogel was in two distinct states. When in the pre-MA state, the hydrogel is in the initial stages of the trial, with ions still

aligning to an almost homogeneous distribution and not yet subject to significant shape change within the EAP. When in the post-MA state, the hydrogel's distribution is considerably altered by the ion migration- and stimulation-induced shape change. Therefore, there is no one-to-one relationship between data points in the two states. Because of this, the statistical significance can be assessed via the p value of sample comparison, using the critical limit theorem and the Mann-Whitney U test. Details on this calculation can be found in Note S5.

These calculations give $p = 0.00041$, placing the probability below 0.05% and rejecting the null hypothesis. This validates the improvement before and after MA as statistically significant, despite any fluctuations between experimental runs, and reinforces the observed increase in hydrogel paddle control ability in the Pong game environment, showing that the improved hit rate, shown in Figure 7A, was not region exclusive but contributed to improved overall game performance.

It can also be observed that the peak in rally length aligns with the average peak in hit rate at approximately 1,600 s, as shown in Figure 7A, with a slight delay of around 150 s. This delay makes sense, as the effect of the improved hit rate would take some time to translate to an improvement in rally length due to the additional layer of abstraction caused by the time taken for a full rally to be completed. Further to this, the average peak in hit rate observed in Figure 7A aligns with the peak electric current measurement observed in Figure 6, with another delay of around 600 s.

This increase in electric current represents the ion distribution of the hydrogel being influenced by the received environmental data, filling the memory similarly to how the memory component was observed in the first section of this paper as electric current measurement. As with the delay between hit rate and rally length, it would take some time for the base-level electric current measurements to translate to improved hit ability due to the layers of abstraction caused by the mechanics of the game and MEA interface.

Last, an additional metric was recorded as rally aces, representing the number of times the paddle failed to intercept the ball without a single hit. The graph of this metric is shown in Figure 7B. This graph shows a clear drop in the number of aces aligning with the points of maximum performance, as found from the previous metrics of hit rate and rally lengths, occurring at 1,706 s. This shows an increase in performance at the same point as the rally lengths. It should, however, be noted that the rally aces before and after MA are very low, below 0.3, despite the further reduction at the point of maximum performance. This indicates that the performance improvement is considerably more visible in rally lengths as opposed to rally aces, possibly due to the frequency and range of available data in the two metrics. The combination of these three metrics shows a clear tendency for performance to increase throughout the course of the game.

Control experiments via interference of information translation. Results from the control experiments were collected, as described in the experimental procedures, to further show that the hydrogel's improved performance was a direct result of accurate environmental information fed into the hydrogels. The control experiments interfered with the translation of information, as shown in Figure 5. The first control experiment interfering with sensing at point 1 was referred to as impaired sensing, the second control experiment interfering with stimulation at point 2 was referred to as impaired stimulation, and the third control experiment severing the stimulation at point 2 was referred to as severed stimulation.
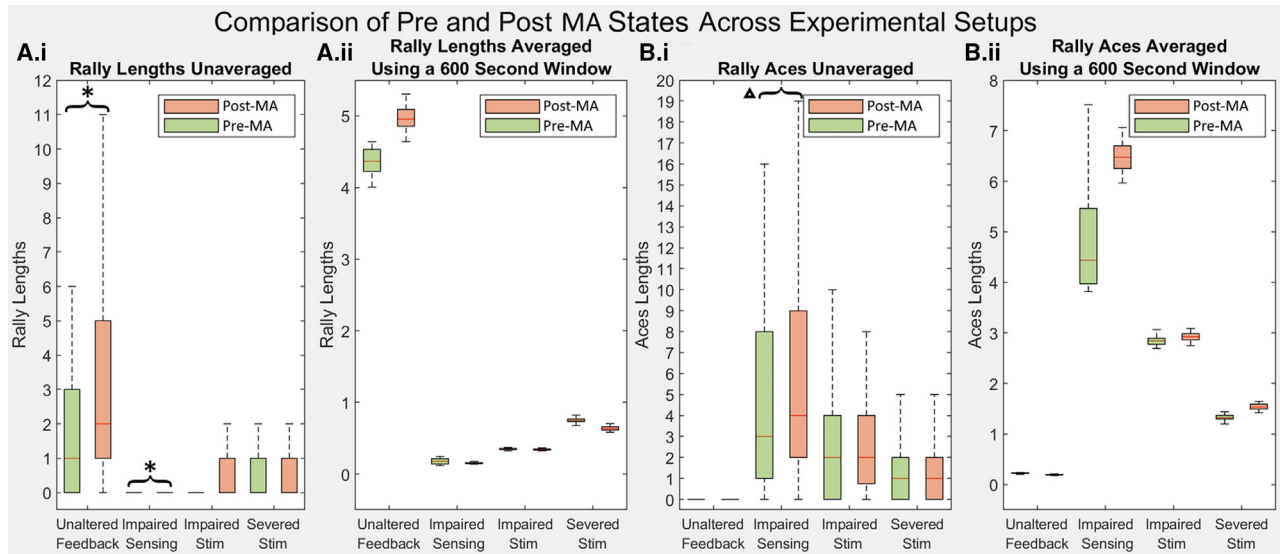
Figure 8. Comparison of pre- and post-MA states across experimental setups

Shown is the comparison of pre-MA and post-MA datasets for each experimental set: unaltered feedback, impaired sensing, impaired stimulation, and severed stimulation. The datasets are sampled from the experimental runs using the same time spans as used for the t test analysis and taken from both the unaveraged discreet dataset and the smoothed average dataset. The averaged dataset was smoothed using a moving average window of 600 s as used in previous analyses. On each box, the central mark indicates the median, and the bottom and top edges of the box indicate the 25th and 75th percentiles, respectively. The whiskers extend to the most extreme data points not considered outliers. The datasets that were shown to be statistically different, via t test, with 0.05% similarity are marked with an asterisk datasets with 0.07% similarity are marked with Δ.

(A.i) Boxplot of rally lengths unaveraged. The unaltered feedback experiment shows an increase in performance as the rally lengths increase between sets. All other experiments show little to no change between pre-MA and post-MA states, representing no improvement in performance.

(A.ii) Boxplot of rally lengths averaged. The unaltered feedback experiment shows an increase in performance as the rally lengths increase between sets. All other experiments show a slight decrease in performance as rally lengths reduce.

(B.i) Boxplot of rally aces unaveraged. The unaltered feedback experiment shows no increase in performance as the rally aces stay approximately 0. All other experiments show either no change between pre-MA and post-MA states or a reduction in performance as rally aces increase.

(B.ii) Boxplot of rally aces averaged. The unaltered feedback experiment shows a very slight increase in performance as the rally aces decrease. The impaired sensing experiment shows a significant decrease in performance as rally aces increase. All other experiments show a slight reduction in performance as rally aces increase.

The hit rate and rally length plots for the first, second, and third control experiment can be seen in Figures S15–S17, respectively. These results are summarized in box-plots shown in Figures 8A.i and 8A.ii. These plots show the distribution of rally lengths in both the pre-MA and post-MA states. As the rally length is an integer, the distribution is discreet and lacks the resolution to show small changes between states; for this reason, the smoothed dataset, as shown in Figure 7A, was also included. The plots show the median as a red line, with the box edges corresponding to the 25th and 75th percentiles and the whiskers showing the maximum and minimum values, discounting outliers. Outliers are defined as 1.5 times the interquartile range away from the bottom or top of the box. The datasets for these states were extracted from the full experimental data for each experiment, following the same procedure as for the t test described in Note S4. As with the unaltered feedback experiment, the stabilization of the standard deviation in the recorded hit rate of the datasets was analyzed to ensure that the number of experiments run was sufficient. The plots of these standard deviations over time with varying dataset sizes can be seen in Figures S11–S13 for the first, second, and third control experiment, respectively.

In Figure 8A.i, it is clear that the rally length for each control experiment is far below that of the original, unaltered feedback experiment. The best performance in the

Pong game was demonstrated based on the closed sensory-motor loop with accurate information of the game environment. Note here that, at the beginning of the Pong game, labeled as the pre-MA state, the unaltered feedback condition already shows higher performance, indicating immediately improved performance as a result of the inference function. In addition, comparing the rally lengths, in Figure 8A.i, for the pre-MA and post-MA states, it can be seen that emergent memory occurs as a function of time. The impaired sensing experiment shows the rally lengths to barely reach beyond 0, showing no improvement in performance. Similarly, the severed stimulation also shows no improvement in performance but is able to achieve rally lengths up to 2, although this is still far below the unaltered experiment.

Interestingly, the impaired stimulation shows an increase in performance, although the achieved rally lengths in the post-MA state are still far below those of the unaltered experiment, and the degree of improvement is far less. Figure 8A.ii shows much of the same; however, the decrease in performance of the control experiments becomes clearer as the data are presented over the non-discreet space. Each of the averaged datasets shows a slight decrease in performance as the rally lengths decrease. However, as these differences only present clearly on the averaged dataset and are only slight, further analysis is required to ensure their statistical significance.

To confirm the statistical significance of the difference in pre-MA and post-MA states within the control experiments, a series of t tests was performed. The tests were performed on the unaveraged dataset to better represent the collected data, using the same method as for the unaltered feedback experiment earlier in this study, as detailed in Note S5. The results of this test are found in Table S1. These results show that, through all experiments, only the pre-MA and post-MA states in the unaltered feedback and impaired sensing experiment present a p-value of under 0.05 and, thus, a statistically significant difference. The Pong game performance, between the pre-MA and post-MA states, for the impaired and severed stimulation experiments was not statistically different. This means that the initially observed reduction in performance, and thus the impact of memory on said performance, is not significant. The lack of performance supports the initial theories of how the altered feedback of information from the environment affects the impact of memory on the hydrogel's behavior.

To further support these conclusions, rally aces were plotted for all control experiments. These can be found in Figures S18–S20 for the inhibited sensing information, inhibited stimulation information, and severed stimulation information, respectively. These results are also summarized in a boxplot shown in Figures 8B.i and 8B.ii, utilizing the same separation of pre-MA and post-MA datasets.

As shown in Figure 8B.i, the control experiments clearly show low performance, with the average rally aces presenting much higher than in the unaltered experiment, in both pre-MA and post-MA states. The rally aces of the unaltered feedback experiment are much too small to be shown on this graph, attributed to the much higher performance; however, because of this, there is little observable change between pre-MA and post-MA states. The impaired sensing experiment, however, shows a clear decrease in performance as rally aces increase. The impaired stimulation experiment shows a similar low performance with high rally aces, although the range narrows. The severed stimulation experiment shows little change between states on this scale; this indicates that there was no decrease in performance but also no

increase similar to the boxplot of rally lengths for the same experiment shown in Figure 8A.i. Figure 8A.ii, as with the rally lengths, shows much of the same; however, a slight decrease in rally aces is visible in the unaltered feedback experiment, aligning with the increased performance shown in rally lengths. Additionally, each of the impaired and severed stimulation experiments shows a slight increase in rally aces over time, indicating a decrease in performance.

As with the rally lengths, the statistical significance of the difference in pre-MA and post-MA states within the rally aces for the control experiments was assessed with a t test, using the unaveraged dataset. The results of this test can be found in Table S2. These results, however, showed no significant statistical difference between pre-MA and post-MA states. This is likely because the rally aces resulted in a reduced range of values compared to the rally lengths and, thus, smaller differences between states, resulting in less significant differences between datasets. However, the impaired sensing does show the most significant difference between states with a p value of 0.07; although this is not conclusively significant, it does enforce the impact of the altered sensing feedback loop on the hydrogel performance in the game.

According to both the rally lengths in Figures 8A.i and 8A.ii and the rally aces in Figures 8B.i and 8B.ii, it is clear that the performance of the impaired sensing experiment is far worse than in the other control experiments and shows some reduction in performance over the game.

First, in the case of the impaired sensing experiment, the hydrogel "memorizes" the correct environmental data, but the interpretation of those data is incorrect. With the hydrogel's sensing regions rearranged, the hydrogel's motor commands to control the paddle are incorrect. Thus, the paddle was moved incorrectly, demonstrating poor performance. As MA continues, this performance worsens as the paddle is moved more precisely but with the continued incorrect interpretation.

Second, in the case of the impaired stimulation experiment, even with the incorrect environmental information (represented by incorrect the ball position in the game environment), the hydrogel was provided electric stimulation via the rearranged stimulation electrodes. This means that the hydrogel was still adapting, as the ions moved to a distribution representative of the provided stimulation. Unfortunately, as the information that the provided stimulation represents was wrong, the information acquired by the hydrogel was also wrong, and performance decreased.

Third, in the case of the severed stimulation experiment, the hydrogel no longer received any environmental information, so no stimulation was provided to the hydrogels. Based on the electric current recording from the hydrogels, the motor commands were produced to control the paddle, but as no electric stimulation was provided, the hydrogels were effectively "blinded." This lack of meaningful information resulted in a slight reduction in performance as the hydrogel was unable to adapt to the simulated environment in any meaningful way. This open loop experiment further confirms the importance of the closed loop in the unaltered feedback experiments.

These observations help to reinforce that the hydrogel's increase in performance is directly related to accurate representation of the virtual environment in which it is acting. A more detailed analysis of the specific hit rate, rally length, and rally ace line plots can be found in Note S8.

Cell Reports
Physical Science
Article

Game world performance in relation to memory functions via ion migration and free energy. With the significance of the observed performance increase within Figures 7A and 7B confirmed via comparison with the control experiments, there is a clear performance improvement or memory mechanism at play. In this section, we discuss the way in which the hydrogel dynamics, through free energy minimization via ion migration, result in this emergent memory and adaptation. In other words, how does the change in free energy as a result of polymer and ion dynamics (electrostatic interactions between polymers and ions, physical entropy of polymer networks, ion migration, etc.) alter the paddle's behavior with respect to ball position and result in increased game performance and emergent adaptation via memory?

The molecular picture of the free energy is extremely complex, as the already complex EAP system (charged polymer networks interacting with ions and water molecules)[38] is, in this study, open and coupled to the environmental dynamics of the Pong game through the electrostatic forces applied externally.

To summarize free energy in the context of the EAP hydrogel, minimization results from the equalization between three main sources of free energy, as shown in Equation 2. These are free energy on ions due to the electric field, free energy due to the chemical gradient of ions and water molecules, and free energy due to the electrical gradient of ions. The electric field application causes a gradient of increased free energy, shifting the equilibrium state.

The game environment closed loop can be summarized as measured electric current encoded into paddle motor commands and the ball's position fed back via electric stimulation to the hydrogel. As the ions migrate to minimize free energy, under the electric field, the redistribution of ions affects the game environment through paddle motion since the paddle's motion alters the ball's trajectory through collision.

To develop the chain of events that culminate in improved performance, the kinematics of the paddle were analyzed over the course of the game through analysis of the changing distribution of paddle positions over time. This can be approached by analyzing the paddle's motion in response to the ball's location. This analysis is detailed in Note S6.

Both the paddle and ball move on the y axis, each vertical position in which the paddle or ball exists can be thought of as a state of the paddle or ball. By applying a window to the data, the change in positions can be shown as changing state distributions through the course of the game.

Figure 9A shows the mean of the paddle positional state probability distributions as a function of time. Individual distributions can be seen in Figure S9, showing probability distributions for timestamps 200, 400, 600, 800, 1,000, 1,200, 1,400, 1,600, 1,800, and 2,000. In these figures, there is a clear change in the distribution of paddle positions as the game progresses. Initially starting with a large central peak that becomes less pronounced as the gel reaches its maximum performance point at 1,800 s, as shown in Figure 7A, where the distribution becomes more uniform. From this, it can be deduced that the distribution of paddle positions changes through game play. In line with the principles of free energy, this distribution of states can be thought of as a memory function. The distribution represents the ball's motion within the simulation environment and is represented by the ion distribution within the polymer network.
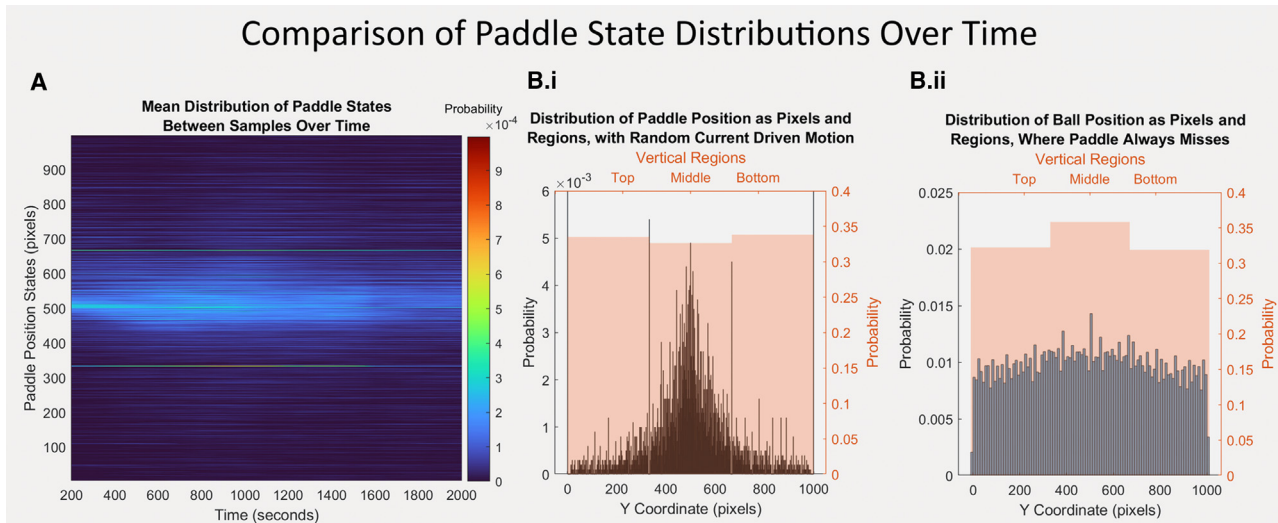
Figure 9. Comparison of paddle state distributions over time

(A) The mean distribution of paddle states for all 21 experimental samples as a heatmap. Distributions were sampled every 20 s starting at t = 100 using a window of 200 s, providing enough data points for accurate representation with minimal sample overlap. The color of each point represents the state probability. States of 0 and 1,000 pixels were omitted; the probability of these states was much higher that of than others (0.0129 and 0.0177 respectively) due to the boundary conditions and so would obscure the data by scale biasing. An additional set of plots can be seen in Figure S9, showing individual distributions for the timestamps 200, 400, 600, 800, 1,000, 1,200, 1,400, 1,600, 1,800, and 2,000.

(B) Distributions of positional states from paddle and ball simulations. Each plot shows the distribution divided into bins of each state, signified by the blue bars, and divided by regions shown by the orange transparent overlay bars.

(B.i) The simulated distribution of paddle states generated, using the algorithm described in Figure 4C, with randomized electric current values. 10,000 samples were simulated to show the distribution. To allow the central peak to be visible, the left y axis was limited to 0.006; however, the states of 0 and 1,000 are higher than the central peak due to the boundary conditions. The states 0 and 1,000 have probabilities of 0.2754 and 0.2796, respectively.

(B.ii) The simulated distribution of vertical ball states using the maximum hit rate for each region. The ball was simulated with the same game physics, starting with a random direction and resetting to the center on a miss. The probability of the ball being intercepted by the paddle was recorded as 0.98, 0.58, and 0.86 for the top, middle, and bottom regions, respectively. Each time the ball hit the paddle wall in simulation, these probabilities were used to simulate whether the ball hit the wall or paddle. As the ball moved, the full path of each ball simulation was recorded, resulting in 600,000 samples, with the travel of each ball simulation before reset lasting, on average, 245 samples.

In Figure 9A, the states of y = 0 and y = 1,000 were omitted, as their larger values obscured the rest of the results. These larger values are a result of the boundary conditions. To fully explore the memory mechanics, the impact of these boundary conditions must be investigated.

The boundary conditions occur because the paddle cannot pass beyond the edge of the game environment. If the measured electric current trend used to place the paddle, as shown in Figure 4C, has a positive gradient toward either edge, the paddle will be placed at the edge. This means that there are more combinations of electric current that lead to the paddle being at the edges than in between. The boundary conditions can be visualized by simulating the paddle with random electric current inputs, using the algorithm described in Figure 4C, and recording the paddle's positional states. A distribution of these simulated results is shown in Figure 9B.i; this plot shows that, with random electric current, the paddle has a significant tendency toward either end, with a peak distribution in the center. The shape of distribution at the center can also be explained as a result of the boundary conditions and is analogous with a depletion force. The boundaries in the paddle's motion act as two point forces with high attraction to the paddle; the forces interact at the mid-point between them, creating a peak.[57,58] With greater resolution, the effect of the boundary conditions could be reduced. However, that is beyond the scope of this study. The distribution shown in Figure 9B.i is similar in shape to the initial distribution at

t = 100 in Figure 9A, as the paddle's initial motion is almost entirely influenced by the boundary conditions having yet to gather enough information to diverge.

Although the boundary conditions explain the initial state distribution of the paddle, to understand the change in behavior, the distribution at maximum performance (t = 1,800) must be assessed. If the paddle's state distribution represents the "memorized" knowledge about the environment, and the ball's state distribution represents the actual environment, a system that is adapting its behavior based on memory would seek to minimize the difference between these distributions.

Indeed, in an ideal Pong game, the paddle position should match that of the ball's vertical position. Ideal anticipation of ball dynamics would mean that the paddle's position would be the same as the ball's position once it hits the wall. Essentially, the paddle's vertical position would match that of the ball's vertical position with a time offset in relation to the proximity of the ball to the paddle, defined by the degree of anticipation. This means that the paddle and ball should move through the same positions over the course of the game, meaning that the ball and paddle should have almost identical distributions of vertical positional states.

By comparing the paddle's state distribution against that of the ball, the paddle's change in behavior can be assessed against what would be the ideal behavior, and the impact of memory on the hydrogel's embodiment within the simulated environment can be contextualized. This allows analysis of what attributes of the paddle's distribution change to match that of the ball, leading to improved performance. The ball's state distribution can be simulated using the Pong game environment. However, the ball resets on missing the paddle, which alters the ball's distribution. This means that, as performance improves, the ball's behavior changes as it is hit more and follows different trajectories. This is evident when comparing two simulations of the ball's positional distribution, where the ball is never hit by the paddle and where it is always hit by the paddle, as shown in Figures S14A and S14B. To accurately compare the paddle's distribution to that of the ball, the ball's distribution must represent the behavior of the ball at the point of maximum performance. At this point, the hit rates are 0.98, 0.58, and 0.86 for the top, middle, and bottom regions, respectively, as shown in Figure 7A. When the ball hits the paddle wall, the ball is either bounced (as if hit by the paddle) or reset (as if hitting the wall) according to the hit rate of the region in which it hits the paddle wall; this simulated distribution can be seen in Figure 9B.ii. From this distribution, the ball's vertical motion over the game environment is more uniform than the paddle's initial distribution with fewer unique states (represented as the number of histogram bins), indicative of the predictable ball trajectories. As shown in Figure 9A, the paddle's distribution appears to become more uniform as the central peak becomes less pronounced. Additionally, the number of unique states reduces, also moving closer to the ball's distribution. These observations, however, need to be quantified via metrics representing the behavioral change of paddle and ball motion as a result of the closed-loop interaction with them.

There are two main metrics used to analyze the attributes of the paddle and ball motion distribution, both representative of information entropy within the system used to quantify the impact of memory on the behavior of the EAP hydrogel.

(1) Number of unique states: the number of unique states/positions in which the paddle/ball is recorded within the sample window used to generate the distribution (also represented as the number of histogram bins). Defined

in Equation 7 as o, where Q is the sample used to make the distribution, O is the set of elements in Q without repetitions, and $|O|$ represents the cardinality of O. When applied to the ball, due to the resolution of the ball's motion as applied to the gel, the number of unique states of the ball will remain constant, limited by the 6 regions the ball inhabits, so not providing usable information. Information entropy S is a function of unique states u. In statistical thermodynamics, physical entropy is defined as $S = k_B \ln \Omega$,[59] where k_B is the Boltzmann constant and Ω is the number of microstates. As the paddle position is determined by conductivity of ions and their distribution, the physical entropy of the hydrogel is fundamentally linked to the information entropy of the paddle states, as Ω influences unique states u.

(2) Variance in frequency of unique states: the variance in quantity of occurrence of each unique state, used as a measure for uniformity in the distribution; defined in equation set (6) as σ^2, where c_i is the number of occurrences of the ith element of O, $bar c$ is the mean value of c, Q_j is the jth element of Q, and q is the number of elements in Q. Shown in Figure 9B.i, the boundary states of 0 and 1,000 greatly overshadow the central peak distribution. As the edge conditions are results of the interfacing algorithm and only represent a fraction of the paddle's motion, they can be ignored for the purposes of calculating variance in the paddle. This allows the uniformity in the central peak to be more accurately compared to that of the ball that is not subject to boundary conditions, as shown in Figure 9B.ii. Variance is linked to information entropy through information theory. Although not directly proportional, information entropy and variance are both measures of expected values and share trend directionality[60]:

$$\sigma^2 = \frac{\sum (c_i - \overline{c})^2}{o - 1} \qquad \text{(Equation 6)}$$

$$o = |O| \qquad \text{(Equation 7)}$$

where:

$$c_i = \sum_{j=1}^{q} f(Q_j, O_i)$$

$$f(Q_j, O_i) = \begin{Bmatrix} 1 & Q_j = O_i \\ 0 & Q_j \neq O_i \end{Bmatrix}$$

Due to the dynamic nature of the hydrogels, each sample will have slight variations in ion distribution, polymer density, and surface texture; this could lead to differences in recorded metrics. However, the emergent memory behavior is still driven by the same mechanics regardless of starting inconsistencies, and, as a result, the trend's shape of these metrics will be consistent between samples. To minimize the effect of gel synthesis inconsistencies, the metrics are normalized via feature scaling to better highlight the shape of the trends. The plot of these trends is shown in Figure 10. The lines represent the mean between all samples, with error bars representing the standard error between all samples used.

(1) At t = 200, the number of unique paddle states is low, while the variance in both paddle and ball is high, showing few states with large variations in frequency. This matches the simulated distribution shown in Figure 9B.i, as expected, as the initial distribution will be almost entirely driven by the

Cell Reports
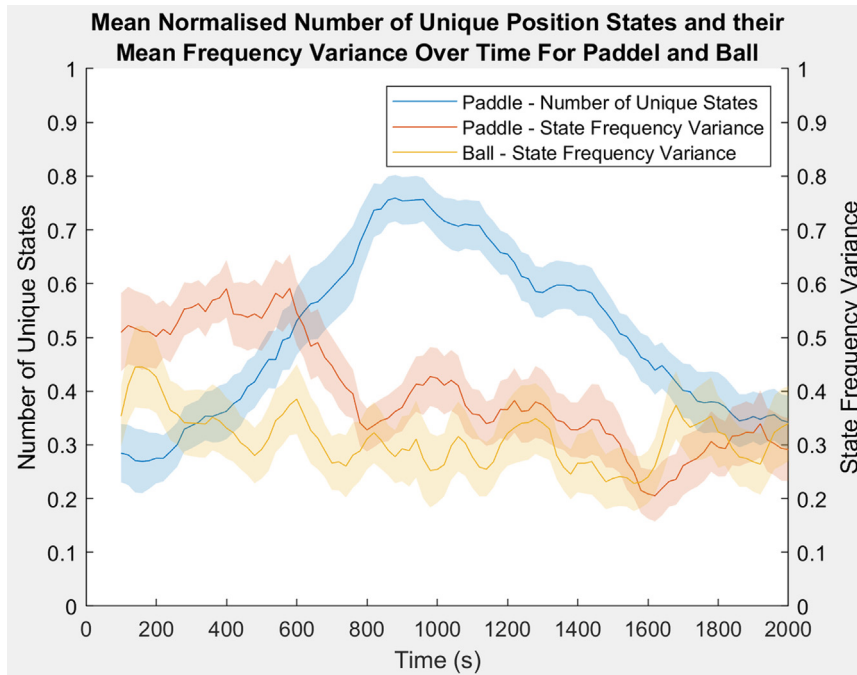**Physical Science**
Article

CellPress
OPEN ACCESS

Figure 10. Mean of the normalized number of unique paddle states and the mean of the normalized variance between unique paddle state frequencies for both the paddle and ball over the course of the game

Distributions were generated from each gel sample using a window size of 200 s, as in the plots in Figure 9A, sampled every 20 s from t = 100 to t = 2,000. The number of unique paddle states and state frequency variance were then normalized, and the mean between gel samples was found. The standard error between gel samples is shown by the shaded area.

boundary conditions, as no information has been gathered about the game environment, and ions remain in a homogeneous distribution.

(2) At t = 600, the number of states increases as the variance decreases in both paddle and ball. This happens as more information about the environment is gathered and coincides with the rise in electric current, as shown in Figure 6. With the application of an electric field, the ions start to migrate within the hydrogel to represent the stimulation. As ion mobility increases, the number of unique states increases, and the paddle explores more of its working area. Simultaneously, as more of the working area is explored, paddle motion becomes more evenly distributed, and so the variance decreases. As the ball is hit more often, its variance decreases as it moves through more of the game environment before being reset on a miss. This is evident when comparing variance of simulations where the paddle always hits and always misses the ball, as shown in Figures S14A and S14B.

(3) At t = 1,000, the number of states reaches its maximum and starts to decrease; this coincides with the behavior of the electric current, as shown in Figure 6, and can be explained though ion mobility. Initially, the ions have total mobility, as the gel is yet to change in structure; as the ion mobility increases, hysteresis takes effect within the hydrogel, opposing ion migration. Eventually, ion mobility reaches its maximum, causing the maximum peak in electric current shown in Figure 6. After this point, the hysteresis effect continues, and ion mobility decreases, causing the number of unique states to decrease, as ions start to settle into their final positions.

CellPress
OPEN ACCESS

(4) At t = 1,800 both the number of states and variance in the paddle have reached their minimum; this coincides with the point of maximum performance shown in Figure 7A. The normalized variances in paddle and ball now match, as the paddle and ball behavior have a stronger coupling. As the memory continues to saturate, the ion distribution comes to better represent the ball's motion. This leads to reduced paddle state variance and reduced number of unique paddle states, causing the behavior of the paddle to become more like that of the ball. This causes the ball to be missed less often, resulting in a more homogeneous distribution of ball states and less variance, as seen in Figure S14B. The saturation of memory is caused by the hysteresis and so is linked to the breakdown of the polymer structure. Eventually, the same mechanic that allows the gel to retain memory causes the polymer structure to beak down to a point where it inhibits conductivity and performance reduces.

The trends shown in Figure 10 and the way in which they coincide with features in other figures add another step to the chain of events leading to increased performance. This highlights interesting forms of emergent behavior occurring as the ions migrate to reduce free energy.

Interpretation
As seen through the experimental results, there is a clear increase in performance of the EAP hydrogel to play the Pong game, as shown in Figure 7A, when given information that is representative of the virtual game environment. This improved performance directly results from the MA of environmental information without the presence of active feedback via a reward/punishment system as present in BNN systems. Over the course of the game, the ball and paddle inhabit more areas of the game environment, resulting in more environmental information influencing memory via stimulation of the polymer structure. In this way, the hydrogel gathers information about the environment and, through this collection of information, improves in performance. The positive impact of memory on EAP hydrogel performance is possible due to the inference function defined in the encoding from hydrogel output to paddle position, shown in Figure 4C. The inference function is how the error between internal states, of the ion distribution, and external states, of game dynamics, are applied to actions of moving the paddle, similar to that of unsupervised learning algorithms.

The development of the increased performance, based on the paddle state dynamics, can also be directly linked to the underlying mechanics of the EAP hydrogel through ion migration and memory mechanics due to hysteresis. Through this linking, it can be theorized that, via physical entropy of ion distribution and information entropy of paddle states, an initial logical similarity can be established between the properties of EAP hydrogels and computational information theory.

To contextualize the active medium's interaction with the simulated environment within the control loop, external states of the environment influence internal states of the active medium. In the case of this study, the EAP hydrogel achieves this through a looped exchange of information called comparable to active inference. Active inference is a common theory of learning within the study of BNNs, often conceptualized through free energy minimization and FEP. Active inference analogizes an internal generative pseudo-model used to predict inputs that represent the external world,[23,27,28] based on theories of Bayesian inference.[61,62] Similarly, comparisons to theories of criticality can also be drawn. Criticality theorizes that

learning coincides with reorganization of the active structure, and hydrogel presents reorganization or restructuring via the ions and charged polymer networks. This reorganization could be described as an induced phase transition when the system is provided energy via applied external stimulation, in line with a simplified view of theories of criticality. Figure 6 shows an increase in electric current level, as provided by the stimulation, that coincides with improved performance, as shown in Figures 7A and 7B. However, the comparison to theories of BNN learning falls beyond the scope of this study but provides an interesting avenue of exploration in future work.

It is clear from Figure 10 that the minimization of the unique number of states and state frequency variance in both paddle and ball coincide with improved performance. In Figure 10, the state frequency variance of both the paddle and ball become closer as performance increases. This quantization of information entropy is representative of the hydrogel memory, linked to ion distribution; as information is collected, the memory becomes saturated, leading to less impact on the overall system. Similarly, the minimization of both measurements of information entropy align with the minimization of free energy resulting within the EAP hydrogel as ions migrate. These events also align with the simplification of distributions shown in Figure 9A and maximization of accuracy, observed in the improved performance shown in Figure 7A. The parallel events shown here construct an interesting view of the role of memory within the system, highlighting how information provided to the EAP hydrogel emerges within the behavior of said EAP hydrogel via its actions in the simulated environment.

The experimental results, presented in Figure 8, also show that, when an incorrect representation of the virtual environment is provided to the hydrogel or the actions of the hydrogel are altered, the performance is severely inhibited. This behavior can be explained through the memory mechanics as a result of ion interactions and migration. The hydrogel seeks to represent the information given via ion migration. If the environmental information provided to the hydrogel does not accurately represent the environment in which the hydrogel's outputs are being applied, the ions will redistribute to represent this incorrect information.

The implications of these results also support the earlier comparison to unsupervised learning techniques. If the same inference function was used for a different goal, then the performance would decrease. This is because the goal is provided to the hydrogel via the inference function and is how the error between internal and external states is used to alter actions. The control experiments show examples of altering the inference function without altering the goal and the reduced performance that follows.

DISCUSSION

This study applied the theories of memory and computation in BNNs to ionic EAP hydrogels using common mechanics of ion migration and structural reorganization.

First, by measuring ion concentrations through conductivity of the EAP hydrogel after periods of stimulation, the memory mechanics of the ionic EAP hydrogel were highlighted. This provided a basis that was then used in the integration of a closed-loop system in further experimentation.

Second, utilizing techniques in reservoir computing and unsupervised learning, the ionic EAP hydrogel was embodied in the simulated game world of Pong through the

use of a custom MEA. The game environment was encoded into stimulations provided to the hydrogel, and recorded ion concentrations were used as motor commands within the game world. Through analysis of the behavior of the EAP hydrogel within this simulated environment, improved performance was observed through the course of the game. Additionally, through analysis of how performance improvement manifested through behavioral changes, the mechanisms of the EAP hydrogels were linked back to FEP and criticality.

By investigating the chain of events leading from ion migration to game performance, the emergent MA of ionic EAP hydrogels was clarified, showing how the integration of said memory emerged as beneficial behavioral changes in the EAP hydrogel's action within the game. This was achieved by recording information from the various layers of abstraction, from electric field stimulation to rally lengths, and analyzing the connections between these layers. The Pong game acts as a problem to be solved. When this problem is provided to the hydrogel as an electric field, it creates a gradient of increased free energy. Due to the active mechanics of the hydrogel and the memory functions, the hydrogel updates its memory of the environment via ion migration, effectively gaining information about the environment in which it is embodied. The ions within the hydrogel seek to minimize the free energy gradient caused by the electric stimulation and redistribute; the redistribution of ions then becomes the solution to the problem. This minimization of free energy coincides with an increase in relative energy within the system and could be linked to current theories of learning in BNNs through future work.

The way in which the solution is interpreted allows it to be applied to the problem; in this case, through conversion of localized ion concentration to paddle motion. As ions migrate to represent the game environment, presented as a series of changing electric fields, the memory in the hydrogel is filled, resulting in an increase in electric current draw. This then causes a change in paddle motion to better intercept the ball, which, in turn, improves the hit rate in the regions, which, in turn, increases the rally lengths.

The results of this study demonstrate that certain active media, such as ionic EAP hydrogel, whose behavior is driven by mechanisms comparable to those found in computational systems, can be used in similar computational applications. Through the application to such a computational task, using current techniques in reservoir computing, EAP hydrogels were shown to demonstrate an emergent memory-like function that contributed to improved performance within the task. These results show a promising avenue for complex computation achievable within many more active media that also demonstrate similar free-energy-driven mechanisms.

Future work

This study demonstrated that a form of emergent memory and adaptation, when embodied in a computational task, is possible in media other than BNNs, when the behavior of the medium in question is also subject to the principles of free energy. However, as an initial study of this behavior, the experimental setup used does not achieve the same spatial resolution that has been achieved with BNNs using high-density MEAs. In future work, higher-resolution MEAs can be tested to gain a deeper understanding of the part that free energy and structure reorganization play in the observed memory functions. Furthermore, through the use of a higher-density MEA, comparisons to current theories of learning within BNNs can be explored.

**Cell Reports
Physical Science**
Article

One such theory is that of FEP, which contextualizes the observed memory as a pseudo-internal model that updates with environmental feedback. Although FEP is generally discussed through BNNs, it only occurs in neurons as a network, not individually, associating the learning of neural networks with the framework of the FEP. Comparatively, EAPs are subject to free energy at the more integral physical chemistry level, resulting in greater alignment with FEP and criticality theories. These future experiments would aim to highlight the similarities between the minimization of free energy within the EAP hydrogel and theories of minimization via active inference and FEP using the sensory information for better performance.

Another theory of learning that has shown similarities to the hydrogel's behavior is that of dynamic criticality. Criticality contextualizes the restructuring of the active medium's structure as the generation of long-range signaling pathways, improving sensory-motor information processing. Through understanding ionic mobility and EAP mechanics, the restructuring of the hydrogel, and how this impacts memory, can be described. However, to fully realize the impact of criticality in the possibility of learning, this reorganization would need to be monitored. In a future study, a higher-resolution MEA can also be used to monitor the ion distributions at higher spatial and temporal resolutions. This would allow the emergence of criticality to be studied alongside the demonstrated immediate adaptation and potential learning.

Expanding on this potential for future work, both theories of the FEP and criticality rely on the restructuring of the active medium to result in learned behavior. As sensory inputs influence structural change, the system moves closer to a critical state. The new structure is representative of the sensory inputs and, by inference, is representative of the environment from which the inputs came. Restructuring and criticality present behaviorally as either action to reduce the difference between the internal model and sensed environment by making the environment match the model or by altering the internal model to better reflect the environment. Under this theory, BNNs hold "beliefs" about the state of the environment, and learning behavior emerges by minimizing internal free energy through either updating these beliefs or taking action to change the environment to match these beliefs.[27,63] Simultaneously, it is through the local reduction of free energy and FEP that a critical state is achieved and the actions and changing beliefs can be achieved globally. The aforementioned studies[22,31,36] show these theories to hold merit, as the application of BNNs to the Pong game effectively allowed improved performance over time.[22] However, this learning is fundamentally achieved via FEP and criticality.[23,28] The exploration of these theories of learning could highlight interesting links between current theories of learning within BNNs and links between these theories and other potential media whose mechanics are also driven through free energy and restructuring.

Additionally, the method used in this study did not employ any form of active reward/punishment feedback as many neural based MEA systems do. It is possible that, through the addition of this kind of system, even greater performance could be achieved for a given purpose. Furthermore, additional applications can attempt to investigate how the learning behavior is influenced by task. Investigation of the synthesis procedure would also be a productive avenue of future work, experimenting with alternate polymer structures to expand the lifetime of the hydrogel and, thus, open up its application to additional situations. Expanding on this, free-energy-based mechanics are also found in many other forms of active matter and natural systems. Through exploration of these alternatives, a medium that is more capable, and

just as accessible, could be found. All of these avenues of research, however, fall outside of the goals of this study but describe an interesting path for future work and application of this technology.

EXPERIMENTAL PROCEDURES

Resource availability

Lead contact
Requests for further information, resources, and reagents should be directed to and will be fulfilled by the lead contact, Yoshikatsu Hayashi (y.hayashi@reading.ac.uk).

Materials availability
This study did not generate new unique reagents.

Data and code availability
- All generated data have been deposited at Zenodo under https://doi.org/10.5281/zenodo.12740409 and are publicly available as of the date of publication.
- All original code has been deposited at Zenodo under https://doi.org/10.5281/zenodo.12740409 and is publicly available as of the date of publication.
- Any additional information required to reanalyze the data reported in this paper is available from the lead contact upon request.

SUPPLEMENTAL INFORMATION

Supplemental information can be found online at https://doi.org/10.1016/j.xcrp.2024.102151.

AUTHOR CONTRIBUTIONS

Conceptualization, V.S. and Y.H.; methodology, V.S. and Y.H.; software, V.S.; formal analysis, V.S.; investigation, V.S.; writing – original draft, V.S., Y.H., and W.H.; writing – review & editing, V.S., Y.H., and W.H.; supervision, Y.H. and W.H.

DECLARATION OF INTERESTS

The authors declare no competing interests.

REFERENCES

1. Ruskin, H.J., and Walshe, R. (2006). Emergent computing-introduction to the special theme. ERCIM News *64*, 24–25.

2. Bondar, S., Hsu, J.C., Pfouga, A., and Stjepandić, J. (2017). Agile digitale transformation of enterprise architecture models in engineering collaboration. Procedia Manuf. *11*, 1343–1350.

3. Fernando, C., and Sojakka, S. (2003). Pattern Recognition in a Bucket. In European Conference on Artificial Life (Springer), pp. 588–597.

4. Van der Sande, G., Brunner, D., and Soriano, M.C. (2017). Advances in photonic reservoir computing. Nanophotonics *6*, 561–576.

5. Tero, A., Takagi, S., Saigusa, T., Ito, K., Bebber, D.P., Fricker, M.D., Yumiki, K., Kobayashi, R., and Nakagaki, T. (2010). Rules for biologically inspired adaptive network design. Science *327*, 439–442.

6. Dueñas-Díez, M., and Pérez-Mercader, J. (2019). How chemistry computes: language recognition by non-biochemical chemical automata. from finite automata to turing machines. iScience *19*, 514–526.

7. Wang, A.L., Gold, J.M., Tompkins, N., Heymann, M., Harrington, K.I., and Fraden, S.

Cell Reports
Physical Science
Article

CellPress
OPEN ACCESS

(2016). Configurable nor gate arrays from belousov-zhabotinsky micro-droplets. Eur. Phys. J. Spec. Top. *225*, 211–227.

8. Misra, J., and Saha, I. (2010). Artificial neural networks in hardware: A survey of two decades of progress. Neurocomputing *74*, 239–255.

9. Végh, J. (2019). How amdahl's law limits the performance of large artificial neural networks. Brain informatics *6*, 1–11.

10. Mainzer, K. (2009). From embodied mind to embodied robotics: Humanities and system theoretical aspects. J. Physiol. Paris *103*, 296–304.

11. Cangelosi, A., Bongard, J., Fischer, M.H., and Nolfi, S. (2015). Embodied Intelligence. In Springer Handbook of Computational Intelligence (Springer), pp. 697–714.

12. Müller, V.C., and Hoffmann, M. (2017). What Is Morphological Computation? On How the Body Contributes to Cognition and Control. Artif. Life *23*, 1–24.

13. Shapiro, L., and Spaulding, S. (2021). Embodied Cognition. In The Stanford Encyclopedia of Philosophy, E.N. Zalta, ed. (Metaphysics Research Lab, Stanford University). Winter 2021 edition.

14. Tanaka, G., Yamane, T., Héroux, J.B., Nakane, R., Kanazawa, N., Takeda, S., Numata, H., Nakano, D., and Hirose, A. (2019). Recent advances in physical reservoir computing: A review. Neural Network. *115*, 100–123.

15. Schrauwen, B., Verstraeten, D., and Van Campenhout, J. (2007). An overview of reservoir computing: theory, applications and implementations. In Proceedings of the 15th european symposium on artificial neural networks, pp. 471–482.

16. Heiney, K., Ramstad, O.H., Sandvig, I., Sandvig, A., and Nichele, S. (2019). Assessment and manipulation of the computational capacity of in vitro neuronal networks through criticality in neuronal avalanches in *2019*. In IEEE Symposium Series on Computational Intelligence (SSCI) (IEEE), pp. 247–254.

17. Aaser, P., Knudsen, M., Ramstad, O.H., van de Wijdeven, R., Nichele, S., Sandvig, I., Tufte, G., Stefan Bauer, U., Halaas, Ø., Hendseth, S., et al. (2017). Towards making a cyborg: A closed-loop reservoir-neuro system. In ECAL 2017, the Fourteenth European Conference on Artificial Life, *14*, pp. 430–437.

18. Mateos-Aparicio, P., and Rodríguez-Moreno, A. (2019). The impact of studying brain plasticity. Front. Cell. Neurosci. *13*, 66.

19. Chao, Z.C., Bakkum, D.J., and Potter, S.M. (2008). Shaping embodied neural networks for adaptive goal-directed behavior. PLoS Comput. Biol. *4*, e1000042.

20. Bakkum, D.J., Chao, Z.C., and Potter, S.M. (2008). Spatio-temporal electrical stimuli shape behavior of an embodied cortical network in a goal-directed learning task. J. Neural. Eng. *5*, 310–323.

21. DeMarse, T.B., and Dockendorf, K.P. (2005). Adaptive flight control with living neuronal networks on microelectrode arrays. In Proceedings. 2005 IEEE International Joint Conference on Neural Networks, 2005, *3*Proceedings. 2005 IEEE International Joint Conference on Neural Networks, 2005 (IEEE), pp. 1548–1551.

22. Kagan, B.J., Kitchen, A.C., Tran, N.T., Habibollahi, F., Khajehnejad, M., Parker, B.J., Bhat, A., Rollo, B., Razi, A., and Friston, K.J. (2021). In Vitro Neurons Learn and Exhibit Sentience when Embodied in a Simulated Game-World.

23. Friston, K. (2010). The free-energy principle: a unified brain theory? Nat. Rev. Neurosci. *11*, 127–138.

24. Demekas, D., Parr, T., and Friston, K.J. (2020). An investigation of the free energy principle for emotion recognition. Front. Comput. Neurosci. *14*.

25. Friston, K. (2009). The free-energy principle: a rough guide to the brain? Trends Cognit. Sci. *13*, 293–301.

26. Friston, K., Kilner, J., and Harrison, L. (2006). A free energy principle for the brain. J. Physiol. Paris *100*, 70–87.

27. Parr, T., and Friston, K.J. (2019). Generalised free energy and active inference. Biol. Cybern. *113*, 495–513.

28. Friston, K., Schwartenbeck, P., FitzGerald, T., Moutoussis, M., Behrens, T., and Dolan, R.J. (2013). The anatomy of choice: active inference and agency. Front. Hum. Neurosci. *7*, 7.

29. Isomura, T., Kotani, K., and Jimbo, Y. (2015). Cultured cortical neurons can perform blind source separation according to the free-energy principle. PLoS Comput. Biol. *11*, e1004643.

30. Isomura, T., and Friston, K. (2018). In vitro neural networks minimise variational free energy. Sci. Rep. *8*, 16926.

31. Habibollahi, F., Kagan, B.J., Burkitt, A.N., and French, C. (2023). Critical dynamics arise during structured information presentation within embodied in vitro neuronal networks. Nat. Commun. *14*, 5287.

32. Bak, P. (2013). How Nature Works: The Science of Self-Organized Criticality (Springer Science & Business Media).

33. Bak, P., Tang, C., and Wiesenfeld, K. (1988). Self-organized criticality. Phys. Rev. *38*, 364–374.

34. Bak, P., and Creutz, M. (1994). Fractals and Self-Organized Criticality. In Fractals in Science (Springer), pp. 27–48.

35. Feder, J. (2013). Fractals (Springer Science & Business Media).

36. Isomura, T., Kotani, K., Jimbo, Y., and Friston, K.J. (2023). Experimental validation of the free-energy principle with in vitro neural networks. Nat. Commun. *14*, 4547.

37. Ramaswamy, S. (2010). The mechanics and statistics of active matter. Annu. Rev. Condens. Matter Phys. *1*, 323–345.

38. Tanaka, T., Nishio, I., Sun, S.T., and Ueno-Nishio, S. (1982). Collapse of gels in an electric field. Science *218*, 467–469.

39. Marchetti, M., Joanny, J.F., Ramaswamy, S., Liverpool, T.B., Prost, J., Rao, M., and Simha, R.A. (2013). Hydrodynamics of soft active matter. Rev. Mod. Phys. *85*, 1143.

40. Otake, M., Kagami, Y., Inaba, M., and Inoue, H. (2002). Motion design of a starfish-shaped gel robot made of electro-active polymer gel. Robot. Autonom. Syst. *40*, 185–191.

41. Strong, V., Holderbaum, W., and Hayashi, Y. (2022). Electroactive polymer gels as probabilistic reservoir automata for computation. iScience *25*, 105558.

42. Kürsten, R., Sushkov, V., and Ihle, T. (2017). Giant kovacs-like memory effect for active particles. Phys. Rev. Lett. *119*, 188001.

43. Atkins, P., and De Paula, J. (2006). Atkins' Physical Chemistry, *8*.

44. Yashin, V.V., Suzuki, S., Yoshida, R., and Balazs, A.C. (2012). Controlling the dynamic behavior of heterogeneous self-oscillating gels. J. Mater. Chem. *22*, 13625–13636.

45. Kuksenok, O., Yashin, V.V., and Balazs, A.C. (2007). Mechanically induced chemical oscillations and motion in responsive gels. Soft Matter *3*, 1138–1144.

46. De Tommasi, D., Puglisi, G., and Zurlo, G. (2014). Hysteresis in electroactive polymers. Eur. J. Mech. Solid. *48*, 16–22.

47. Bassil, M., Davenas, J., and EL Tahchi, M. (2008). Electrochemical properties and actuation mechanisms of polyacrylamide hydrogel for artificial muscle application. Sensor. Actuator. B *134*, 496–501.

48. Gray, J.R. (2004). Conductivity analyzers and their application. Environ. Instrum. Anal. Handb. *1*, 491–510.

49. Atkins, P., and De Paula, J. (2011). Physical Chemistry for the Life Sciences (Oxford University Press).

50. Atkins, P., Atkins, P.W., and de Paula, J. (2014). Atkins' Physical Chemistry (Oxford university press).

51. Tanaka, T., Fillmore, D., Sun, S.T., Nishio, I., Swislow, G., and Shah, A. (1980). Phase transitions in ionic gels. Phys. Rev. Lett. *45*, 1636–1639.

52. Oyen, M.L. (2014). Mechanical characterisation of hydrogel materials. Int. Mater. Rev. *59*, 44–59.

53. Bourtchouladze, R. (2002). Memories Are Made of This: How Memory Works in Humans and Animals (Columbia University Press).

54. Schiavone, G., Kang, X., Fallegger, F., Gandar, J., Courtine, G., and Lacour, S.P. (2020). Guidelines to study and develop soft electrode systems for neural stimulation. Neuron *108*, 238–258.

55. Jia, K., Li, X., and Wang, Y. (2021). Electrochemical breakdown in hydrogel ionotronic devices. Soft Matter *17*, 834–839.

56. Mathworks, Polyfit. https://www.mathworks.com/help/matlab/ref/polyfit.html, Acessed 05/08/2024.

57. Mao, Y., Cates, M., and Lekkerkerker, H. (1995). Depletion force in colloidal systems. Phys. Stat. Mech. Appl. *222*, 10–24.

58. Lekkerkerker, H.N., and Tuinier, R. (2011). Depletion Interaction. In Colloids and the Depletion Interaction (Springer), pp. 57–108.

59. Schroeder, D.V. (2000). An Introduction to Thermal Physic, *57* (Addison Wesley).

60. Ebrahimi, N., Maasoumi, E., and Soofi, E.S. (1999). Ordering univariate distributions by entropy and variance. J. Econom. *90*, 317–336.

61. Neal, R.M. (2012). Bayesian Learning for Neural Networks, *118* (Springer Science & Business Media).

62. Knill, D.C., and Pouget, A. (2004). The bayesian brain: the role of uncertainty in neural coding and computation. Trends Neurosci. *27*, 712–719.

63. Parr, T., and Friston, K.J. (2018). The discrete and continuous brain: from decisions to movement—and back again. Neural Comput. *30*, 2319–2347.